

AEDC-TSR-88-V32

DTIC FILE COPY

2

INVESTIGATION OF THE DEVELOPMENT  
OF LAMINAR BOUNDARY-LAYER INSTABILITIES  
ALONG A COOLED-WALL CONE IN HYPERSONIC FLOWS

J. C. Donaldson and M. G. Hatcher  
Calspan Corporation/AEDC Operations

December 1988

Final Report for June 20-24, 1988

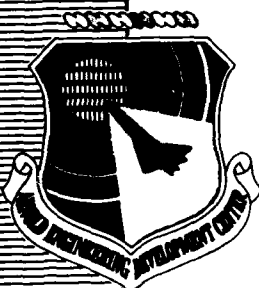
DTIC  
ELECTE  
DEC 21 1988  
S H D

Approved for Public Release; Distribution is Unlimited.

**ARNOLD ENGINEERING DEVELOPMENT CENTER  
ARNOLD AIR FORCE BASE, TENNESSEE  
AIR FORCE SYSTEMS COMMAND  
UNITED STATES AIR FORCE**

88 12 21 001

AD-A202 587



## NOTICES

When U. S. Government drawings, specifications, or other data are used for any purpose other than a definitely related Government procurement operation, the Government thereby incurs no responsibility nor any obligation whatsoever, and the fact that the Government may have formulated, furnished, or in any way supplied the said drawings, specifications, or other data, is not to be regarded by implication or otherwise, or in any manner licensing the holder or any other person or corporation, or conveying any rights or permission to manufacture, use, or sell any patented invention that may in any way be related thereto.

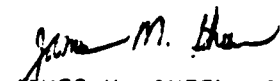
References to named commercial products in this report are not to be considered in any sense as an endorsement of the product by the United States Air Force or the Government.

## DESTRUCTION NOTICE

For classified documents, follow the procedures in DoD 5200.22-M, Industrial Security Manual, Section II-19 or DoD 5200.1-R, Information Security Program Regulation, Chapter IX. For unclassified, limited documents, destroy by any method that will prevent disclosure or reconstruction of the document.


## APPROVAL STATEMENT

This report has been reviewed and approved.

  
JAMES M. GHEEN, Capt, USAF  
Reentry Systems Division  
Dir of Aerospace Flt Dyn Test  
Deputy for Operations

Approved for publication:

FOR THE COMMANDER

  
JAMES G. MILLER, Lt Col, USAF  
Dep Dir, Aerosp Flt Dyn Test  
Deputy for Operations

UNCLASSIFIED

SECURITY CLASSIFICATION OF THIS PAGE

REPORT DOCUMENTATION PAGE				Form Approved OMB No. 0704-0188	
1a. REPORT SECURITY CLASSIFICATION UNCLASSIFIED			1b. RESTRICTIVE MARKINGS		
2a. SECURITY CLASSIFICATION AUTHORITY			3. DISTRIBUTION/AVAILABILITY OF REPORT Approved for public release; distribution is unlimited.		
2b. DECLASSIFICATION/DOWNGRADING SCHEDULE					
4. PERFORMING ORGANIZATION REPORT NUMBER(S) AEDC-TSR-88-V32			5. MONITORING ORGANIZATION REPORT NUMBER(S)		
6a. NAME OF PERFORMING ORGANIZATION Arnold Engineering Development Center		6b. OFFICE SYMBOL (If applicable) DO	7a. NAME OF MONITORING ORGANIZATION		
6c. ADDRESS (City, State, and ZIP Code) Air Force Systems Command Arnold Air Force Base, TN 37389-5000			7b. ADDRESS (City, State, and ZIP Code)		
8a. NAME OF FUNDING/SPONSORING ORGANIZATION AFWAL/FIMG and AEDC/DOF		8b. OFFICE SYMBOL (If applicable)	9. PROCUREMENT INSTRUMENT IDENTIFICATION NUMBER		
8c. ADDRESS (City, State, and ZIP Code) Wright-Patterson AFB, OH Arnold AFB, TN			10. SOURCE OF FUNDING NUMBERS		
			PROGRAM ELEMENT NO. 62201F	PROJECT NO.	TASK NO.
					WORK UNIT ACCESSION NO.
11. TITLE (Include Security Classification) Investigation of the Development of Laminar Boundary-Layer Instabilities Along a Cooled-Wall Cone in Hypersonic Flows					
12. PERSONAL AUTHOR(S) Donaldson, J. C., and Hatcher, M.G., Calspan Corporation/AEDC Operations					
13a. TYPE OF REPORT Final		13b. TIME COVERED FROM 6/20/88 TO 6/24/88		14. DATE OF REPORT (Year, Month, Day) December 1988	
				15. PAGE COUNT 52	
16. SUPPLEMENTARY NOTATION Available in Defense Technical Information Center (DTIC).					
17. COSATI CODES			18. SUBJECT TERMS (Continue on reverse if necessary and identify by block number)		
FIELD	GROUP	SUB-GROUP			
20	04		hypersonic flow boundary layer stability		
14	02		wind tunnel tests hot wire anemometry		
			cold wall model sharp cone (A121)		
19. ABSTRACT (Continue on reverse if necessary and identify by block number) Measurements of fluctuating flow and mean flow parameters were made in the boundary layer on a cooled wall, sharp 7-deg (half-angle) cone in an investigation of wall temperature effects on the stability of laminar boundary layers in hypersonic flow. The flow-fluctuation measurements were made using constant-current hot-wire anemometry techniques. Boundary-layer profiles and cone surface conditions were measured to supplement the hot-wire data. Testing was done at Mach numbers 8 and 6 with a free-stream unit Reynolds number of 1.0-million per foot. The test equipment, test techniques, and the data acquisition and reduction procedures are described. Analysis of the hot-wire anemometer data is beyond the scope of this report.					
20. DISTRIBUTION/AVAILABILITY OF ABSTRACT <input type="checkbox"/> UNCLASSIFIED/UNLIMITED <input checked="" type="checkbox"/> SAME AS RPT. <input type="checkbox"/> DTIC USERS			21. ABSTRACT SECURITY CLASSIFICATION UNCLASSIFIED		
22a. NAME OF RESPONSIBLE INDIVIDUAL C.L. Garner			22b. TELEPHONE (Include Area Code) (615) 454-7813		22c. OFFICE SYMBOL DOCS

DD Form 1473, JUN 86

Previous editions are obsolete.

SECURITY CLASSIFICATION OF THIS PAGE

UNCLASSIFIED

## CONTENTS

	<u>Page</u>
NOMENCLATURE . . . . .	2
1.0 INTRODUCTION . . . . .	7
2.0 APPARATUS	
2.1 Test Facility . . . . .	8
2.2 Test Article . . . . .	8
2.3 Flow-Field Survey Mechanism . . . . .	9
2.4 Flow-Field Survey Probes . . . . .	10
2.5 Test Instrumentation . . . . .	10
3.0 TEST DESCRIPTION	
3.1 Test Conditions and Procedures . . . . .	12
3.2 Data Acquisition . . . . .	14
3.3 Data Reduction . . . . .	16
3.4 Measurement Uncertainties . . . . .	18
4.0 DATA PACKAGE PRESENTATION . . . . .	19
REFERENCES . . . . .	20

## ILLUSTRATIONS

### Figure

1. AEDC Hypersonic Wind Tunnel (B) . . . . .	21
2. Model Geometry and Instrumentation Locations . . . . .	22
3. Test Installation . . . . .	23
4. Survey Probe Rake . . . . .	24
5. Probe Details. . . . .	25
6. Typical Results of a Mean-Flow Boundary-Layer Survey . . . . .	27
7. Model Surface Pressure Variation with Angle of Attack . . . . .	30

## TABLES

1. Model Instrumentation Locations . . . . .	31
2. Estimated Uncertainties of Measured Parameters . . . . .	32
3. Test Summary . . . . .	35
4. Estimated Uncertainties of Calculated Parameters . . . . .	39

## SAMPLE DATA

1. Hot-Wire Anemometer Data . . . . .	40
2. Probe Flow Calibration . . . . .	42
3. Flow-Field Survey Data . . . . .	43
4. Model Surface Measurements . . . . .	47
5. Model Surface Heat-Transfer Data . . . . .	48

INSPECTED  
2

<input checked="checked" type="checkbox"/> <input type="checkbox"/> <input type="checkbox"/>
--

Delete the Export Control Statement in this report. It is approved for public release.  
Per Mr. Carlton Garner, AEDC/DOS

By <i>per telecom</i>	
Distribution/	
Availability Control	
Avail and/or	
Dist	Special
A-1	

## NOMENCLATURE

ALPHA	Angle of attack, deg
CONFIG	Model configuration designation
CSF	Schmidt-Boelter gage calibration factor, Btu/ft <sup>2</sup> - sec - mv
CURRENT	Hot-wire anemometer heating current, mamp
DATA TYPE	Code indicating nature of data tabulated:  "2" - Model surface pressure, temperature, and hot-film anemometer measurements  "4" - Mean boundary-layer profile measurements using pitot pressure and total temperature probes  "6" - Probe calibration measurements in free stream  "9" - Hot-film anemometer probe measurements
DEL	Boundary-layer total thickness, in.
DEL*	Boundary-layer displacement thickness, in.
DEL**	Boundary-layer momentum thickness, in.
DEW	Tunnel stilling chamber dew point temperature, °F
DITTD	Enthalpy difference at boundary-layer thickness, DEL, ITTD-ITWL, Btu/lbm
DITTL	Local enthalpy difference, ITTL-ITWL, Btu/lbm
E	Schmidt-Boelter gage output, mv
EBAR	Hot-wire or hot-film anemometer mean voltage, mv
ERMS	Hot-wire or hot-film anemometer output rms voltage, mv rms
ETA	Effective total-temperature probe recovery factor $ETA = (TTLU - T) / (TT - T)$ or $(TTTU - T) / (TT - T)$
F1 - F4	Identification of hot-film anemometer gage
FIL	Identification of data file used for plot
GAGE	Identification for heat-transfer gage

H (TT), HT (TT)	Heat-transfer coefficient based on TT, $QDOT/(TT-TW)$ , Btu/ft <sup>2</sup> -sec-°R
ITT	Enthalpy based on TT, Btu/lbm
ITTD	Enthalpy based on TTD, Btu/lbm
ITTL	Enthalpy based on TTL, Btu/lbm
ITW	Enthalpy based on TW, Btu/lbm
ITWL	Enthalpy based on TWL, Btu/lbm
K	Schmidt-Boelter gage temperature calibration factor, °F/mv
LRE	Local unit Reynolds number, in. <sup>-1</sup>
LRED	Unit Reynolds number at the boundary-layer thickness, DEL, in. <sup>-1</sup>
LRET	Local "normal shock" unit Reynolds number (based on MUTTL), in. <sup>-1</sup>
LRETD	"Normal shock" unit Reynolds number at boundary-layer thickness, DEL, (based on MUTTD), in. <sup>-1</sup>
M, MACH	Free-stream Mach number
MD	Local Mach number at boundary-layer thickness, DEL
ME	Mach number at boundary-layer edge
ML	Local Mach number
MU	Dynamic viscosity based on T, lbf-sec/ft <sup>2</sup>
MUTD	Dynamic viscosity based on TD, lbf-sec/ft <sup>2</sup>
MUTL	Dynamic viscosity based on TL, lbf-sec/ft <sup>2</sup>
MUTTD	Dynamic viscosity based on TTD, lbf-sec/ft <sup>2</sup>
MUTTL	Dynamic viscosity based on TTL, lbf-sec/ft <sup>2</sup>
P	Free-stream static pressure, psia
PHI	Roll angle, deg
POINT	Data point number
PP	Pitot probe pressure, psia

PPD	Pitot pressure at boundary-layer thickness, DEL, psia
PPE	Pitot pressure at boundary-layer edge, psia
PT	Tunnel stilling chamber pressure, psia
PT2	Free-stream total pressure downstream of a normal shock wave, psia
PW	Model surface pressure (at X = 39 in.), psia
PWL	Model wall static pressure used for boundary-layer survey calculations, psia
Q	Free-stream dynamic pressure, psia
QDOT	Heat-transfer rate, Btu/ft <sup>2</sup> -sec
RE	Free-stream unit Reynolds number, in. <sup>-1</sup> or ft <sup>-1</sup>
RE/FT	Free-stream unit Reynolds number, ft <sup>-1</sup>
RHO	Free-stream density, lbm/ft <sup>3</sup>
RHOD, RHD	Density at boundary-layer thickness, DEL, lbm/ft <sup>3</sup>
RHOL, RHL	Local density, lbm/ft <sup>3</sup>
RHOUD	(RHOD) * (UD), lbm/sec-ft <sup>2</sup>
RN	Model nose radius, in.
RUN	Data set identification number
ST(TT)	Stanton number based on stilling chamber temperature (TT), $ST(TT) = \frac{QDOT}{(RHO) (V)(ITT-ITW)}$
T	Free-stream static temperature, °R, or °F
ΔT	Temperature difference, °F
TAP	Pressure orifice identification number
T/C	Identification number of model surface thermocouples of Schmidt-Boelter heat-transfer gages
TD	Static temperature at boundary-layer thickness, DEL, °R

TDRK	Temperature of Druck probe transducer, °F
TG	Schmidt-Boelter gage embedded thermocouple temperature, °R
THETA	Peripheral angle on the model measured from ray on model top, positive clockwise when looking downstream, deg
TL	Local static temperature, °R
TT	Tunnel stilling chamber temperature, °R, or °F
TTD	Total temperature at boundary-layer thickness, DEL, °R
TTE	Total temperature at boundary-layer edge, °R
TTL	Local total temperature, °R
TTLU	Uncorrected (measured) probe recovery temperature interpolated at the pitot probe location, ZP, °R
TTTU	Uncorrected (measured) probe recovery temperature, °R
TW	Schmidt-Boelter heat-transfer gage surface temperature, °R
TWL	Model wall temperature used for boundary-layer survey calculations, °R
TWTR	Water supply temperature, °R
UD	Local velocity component parallel to model surface at boundary-layer thickness, DEL, ft/sec
UE	Local velocity component parallel to model surface at boundary-layer edge, ft/sec
UL	Local velocity component parallel to model surface, ft/sec
V	Free-stream velocity, ft/sec
X	Axial location measured from virtual apex of cone model, in.
XC	Calculated X location of survey station, in.
XSTA	Nominal X location of survey station, in.
ZA	Anemometer probe height, distance to probe centerline along normal to model surface, in.



ZP

Pitot-pressure probe height, distance to probe centerline along normal to model surface, in.

ZT

Total-temperature probe height, distance to probe centerline along normal to model surface, in.

## 1.0 INTRODUCTION

The work reported herein was performed by the Arnold Engineering Development Center (AEDC), Air Force Systems Command (AFSC), under Program Element Number 62201F, Control Number 2404, at the request of the Air Force Wright Aeronautical Laboratory (AFWAL/FIMG), Wright-Patterson Air Force Base, Ohio 45433-6553, and the AEDC Directorate of Aerospace Flight Dynamics Test (AEDC/DOF). The AFWAL Project Manager was Kenneth F. Stetson and the AEDC/DOF Program Manager was Capt. J. M. Gheen. The results were obtained by the Calspan Corporation/AEDC Operations, operating contractor for the Aerospace Flight Dynamics testing effort at the AEDC, AFSC, Arnold Air Force Base, Tennessee 37389-5000. The test was conducted in the AEDC Hypersonic Wind Tunnel B on June 20-24, 1988, under the AEDC Project Number CI24VB (Calspan Project Number V--B-32).

The objective of this test was to investigate the effects of model surface temperature upon the development of laminar boundary-layer flow instabilities for hypersonic speeds. The test was the seventh in a series of cooperative efforts between AFWAL/FIMG and AEDC/DOF, which have investigated various aspects of boundary-layer stability on sharp and blunt cones. Representative documentation of the previous six tests is given in Refs. 1-3. Selected results of the previous tests are presented in Refs. 4-7.

A water-cooled 7-deg (half-angle) cone model was designed and fabricated specifically for the present investigation. The new cone had the same basic geometry as the uncooled cone models used for the first six investigations, for which the model surface was heated to equilibrium temperature in the wind tunnel flow. The present test effort employed only the sharp-nose model configuration.

The principal measurements of this investigation were hot-wire anemometer probe data acquired above the most-windward ray of the model. These data were supplemented by surveys of the model windward boundary layer using pitot pressure and total temperature probes. Model surface pressure, temperature, and heat-flux were also measured. Data were acquired at Mach number 8 for model angles of attack of 0, 4, and 6 deg and at Mach number 6 for zero angle of attack. Testing at both Mach numbers was done at a free-stream unit Reynolds number of 1.0-million per foot. Hot-wire anemometer and total temperature probes were calibrated in the tunnel flow over a range of unit Reynolds numbers, when required.

Inquiries to obtain copies of the test data should be directed to AEDC/DOF, Arnold Air Force Base, Tennessee 37389-5000, or to AFWAL/FIMG, Wright-Patterson Air Force Base, Ohio 45433-6553. A microfiche record has been retained at AEDC.

## 2.0 APPARATUS

### 2.1 TEST FACILITY

The AEDC Hypersonic Wind Tunnel (B) (Fig. 1) is a closed-circuit wind tunnel with a 50-in.-diameter test section. Two axisymmetric contoured nozzles are available to provide Mach numbers of 6 and 8, and the tunnel may be operated continuously over a range of pressure from 20 to 300 psia at Mach number 6, and 50 to 900 psia at Mach number 8, with air supplied by the VKF main compressor plant. Stagnation temperatures sufficient to avoid air liquefaction in the test section (up to 1,350°R) are obtained through the use of a natural gas fired combustion heater. The entire tunnel (throat, nozzle, test section, and diffuser) is cooled by integral, external water jackets. The tunnel is equipped with a model injection system, which allows removal of the model from the test section while the tunnel remains in operation. A description of the tunnel and airflow calibration information may be found in Ref. 8.

### 2.2 TEST ARTICLE

The model used for this investigation (Fig. 2) was a 7 deg (half-angle) cone designed for AFWAL by AEDC and fabricated under contract to AEDC. The model had a virtual axial length of 40.00 in. and a base diameter of 9.82 in. which were the nominal dimensions of the uncooled models used for Refs. 1-3. The new model was composed of three principal components: (1) The nose section was fabricated of 13-8 stainless steel and had a virtual length of 5.659 in. A nominally sharp nose (0.002 in. tip radius) was used in the present testing. Spherically-blunted noses of 0.25-in. and 0.70-in.-radius were also available. There were no provisions in the model design to circulate coolant in the nose section. (2) A thermal insulator made of Micarta® separated the uncooled nose from the cooled frustum of the cone model. The insulator constituted 0.062 in. of the model axial length. On the inside of the assembled model, a portion of the insulator was threaded to serve as a mechanical connector between the nose and frustum components. (3) The frustum section was fabricated of aluminum alloy 6061-T6 and had an axial length of 34.28 in. The frustum was composed of two concentric conical shells with provision for circulating cooling water between the shells. The outer shell had a uniform thickness of 0.125 in. to within approximately 0.2 in. of the forward end of the frustum. The design flow rate of the cooling water was selected in order to maintain a nominally uniform wall temperature around and along the frustum. The design spacing between the shells was varied, as a function of axial station, to achieve the desired water flow rate. The required spacing was achieved by contouring the inner shell. Cooling water was introduced near the upstream end of the frustum and was drained into manifolds through 16 uniformly spaced holes near the base of the frustum. The water channel between the shells was full at all times during testing. The water supply line and two drain lines were installed in the model mounting sting.

The model was instrumented with four pressure orifices, eight Schmidt-Boelter heat-flux gages, and four flush-mounted hot-film anemometer gages. The locations of the orifices and gages are listed in Table 1 and are indicated in Fig. 2. The heat-flux gages were located adjacent to the cooling water and were sealed into the outer shell of the model using a cement epoxy designed for use with aluminum. Leads from the heat-flux gages were sealed into the wall at the base end of the water channel using the same compound. The orifices and hot-film gages at  $X = 39$  in. were located in lands machined in the outer shell and had no potential for water leaks.

### 2.3 FLOW-FIELD SURVEY MECHANISM

Surveys of the flow field were made using a retractable survey system (X-Z Survey Mechanism) designed and fabricated by the AEDC. This mechanism makes it possible to change survey probes while the tunnel remains in operation. The mechanism is housed in an air lock immediately above a port in the top of the Tunnel B test section. Access to the test section is through a 40-in.-long by 4-in.-wide opening which is sealed by a pneumatically operated door when the mechanism is retracted. Separate drive motors are provided to (1) insert the mechanism into the test section or retract it into the housing (Z drive), (2) position the mechanism at any desired axial station over a range of 35 in. (X drive), and (3) survey a flow field of approximately 10-in. depth (Z' drive). A pneumatically operated shield is provided to protect the probes during injection and retraction through the tunnel boundary layer, during changes in tunnel conditions, and at all times when the probes were not in use.

The probes required for flow-field survey measurements were rake-mounted on the X-Z mechanism (Fig. 4) at the foot of the Z' drive strut that was extended or retracted to accomplish the survey. The angle of the survey strut with respect to the vertical was fixed by manually sweeping the strut to the selected angle between 5 deg (swept upstream) and -15 deg (swept downstream) and locking the strut in position. In the present test, the sweep angle of the strut was reset when the model angle of attack was changed in order that the direction of each survey was normal to the model surface.

A sketch of the survey probe rake is shown in Fig. 4. The top and rear surfaces of the rake were designed to mate to the Z' drive strut of the X-Z Survey Mechanism. The rake was provided with four 0.10-in. I.D. tubes through which were mounted the hot-wire anemometer, pitot pressure, and total temperature probes. The fourth tube was used in the present test for housing a "touch-sensor" probe that caused the survey mechanism to halt when the probe made contact with the model surface. The tubes were fitted with clamps attached to the rake to hold the probes in position. One of the probe tubes of the rake was located in a removable section. This feature facilitated the replacement of fragile probes and allowed for critical probe alignments to be made under a laboratory microscope, if required.

## 2.4 FLOW-FIELD SURVEY PROBES

The hot-wire anemometer probes (Fig. 5a) were fabricated by the AEDC. Platinum, 10-percent-rhodium wires, drawn by the Wollaston process, of 20- $\mu$ in. nominal diameter and approximately 140 diameters length were attached to sharpened 3-mil nickel wire supports using a bonding technique developed by Philco-Ford Corporation (Ref. 9). The wire supports were inserted in an alumina cylinder of 0.032-in. diameter and 0.25-in. length, which was, in turn, cemented to an alumina cylinder of 0.9893-in. diameter and 3.0-in. length that carried the hot-wire leads through the probe holder of the survey mechanism.

The pitot pressure probe had a cylindrical tip of 0.022 in. outside diameter and 0.012 in. inside diameter. This tube was telescoped in a succession of larger diameter tubes for support and to simplify the installation in the probe rake of the survey mechanism. A sketch of the pitot probe is presented in Fig. 5b.

The unshielded total temperature probe was fabricated from a length of sheathed thermocouple wire (0.020 in. O.D.) containing two 0.004-in.-diameter wires. The wires were bared for a length of approximately 0.040 in., and a thermocouple junction of approximately 0.008 in. diameter was made. Details of this probe are shown in Fig. 5c.

In addition to the probes used for survey measurements, a "touch-sensor" probe was used to halt the probe drive mechanism prior to contact of the other probes with the model. (See Sections 2.3 and 3.1.) The probe was made by brazing a lead wire to a piece of 0.042-in.-O.D. steel tubing. This tubing was telescoped in a larger diameter tube (0.093-in. O.D.) and electrically isolated from the larger tube using Pyrocera<sup>®</sup> cement. The inner tubing was bent to make contact with the model surface as required. A similar "touch-sensor" wire was attached to the probe shield (Section 2.3) to stop the probe drive mechanism prior to contact of the shield with the model. (See Section 3.1.)

## 2.5 TEST INSTRUMENTATION

### 2.5.1 Standard Instrumentation

The measuring devices, recording devices, and calibration methods for all parameters measured during this test are listed in Table 2. Also, Table 2 identifies the standard wind tunnel instruments and measuring techniques used to define test parameters such as the model attitude, the model surface conditions, probe positions, and probe measurements. Additional special instrumentation used in support of this test effort is discussed in the succeeding subsections.

### 2.5.2 Model Surface Instrumentation

The locations of the model instrumentation are listed in Table 1 and indicated in Fig. 2. The four surface pressure orifices (TAP 1 - TAP 4) on the model had a diameter of 0.047 in., and the pressures were

measured using Druck® transducers. The transducers are included in the Standard Pressure System of Tunnel B.

The eight Schmidt-Boelter heat-flux gages were fabricated by the AEDC. Each gage consisted of a 0.025-in. thick anodized aluminum wafer which was wrapped with 0.002-in. diameter constantan wire. One-half of the wafer was copper-plated, creating a multi-element copper-constantan differential thermocouple. The wire-wound wafer was partially surrounded by an aluminum heat sink, and the top surface of the wafer, adjacent to the air flow over the model, was covered with a thin layer of epoxy and then painted with a high-temperature paint. On the inside of each gage, an iron-constantan thermocouple was used to measure the temperature of the wafer bottom surface. This temperature and the output of the differential thermocouple were used to determine gage surface temperature and the corresponding heat-transfer rate employing laboratory-calibrated scale factors (See Section 3.3.5.). A more detailed description of the Schmidt-Boelter gage is given in Ref. 10.

The four hot-film anemometer gages were fabricated by the AEDC. Details of the fabrication process are as follows. The substrate was a cylindrical Pyrex® glass plug of 0.08 in. diameter and 0.2 in. length. The glass plug was flame-polished on one end to produce a smooth surface. A film was applied on the end of the plug using a commercially available paint composed of platinum particles in a toluene solution. The streamwise length of the film varied from gage to gage between 0.02 and 0.03 in., with a nominal value of 0.08 in. for the width. The platinum film was extended over the edge of the rod and down opposite sides to allow connections to leads. The film was then fired to bond it to the glass substrate. A stranded-wire electrical lead was bonded to the film extension on each side of the glass plug using a conducting silver epoxy, and the assembly was then coated with a high-temperature insulating paint. A shell for the gage was made from a piece of stainless tubing of 0.125-in. outside diameter and 0.25-in. length which was drilled to an inside diameter of 0.09 in. The inside surface of the shell was coated with the high-temperature insulating paint. An insulating ceramic cement was used as a filler to bond the gage assembly in the shell with the film located flush with the end of the tubing.

The hot-film anemometer gages were operated in the constant-temperature mode. Each gage had a dedicated channel of Thermo-Systems, Inc. equipment composed of the following modules: A Model 1054 anemometer, a Model 1056 variable decade,; and a Model 1057 signal conditioner.

### 2.5.3 Hot-Wire Anemometry Instrumentation

Flow fluctuation measurements were made using hot-wire anemometry techniques. Constant-current hot-wire anemometer instrumentation with auxiliary electronic equipment was furnished by AEDC. The anemometer current control (Philco-Ford Model ADP-13) which supplies the heating current to the sensor is capable of maintaining the current at any one of 15 preset values individually selected using push-button switches. The anemometer amplifier (Philco-Ford Model ADP-12), which amplifies

the wire-response signal, contains the circuits required to compensate the signal electronically for thermal lag which is a characteristic of the finite heat capacity of the wire. A square-wave generator (Shapiro/Edwards Model G-50) was used in determining the time constant of the sensor whenever required. The sensor heating current and mean voltage were fed to autoranging digital voltmeters for a visual display of these two parameters and to a Bell and Howell model VR3700B magnetic tape machine and to the tunnel data system for recording. The sensor response a-c voltage was fed to an oscilloscope for visual display of the raw signal and to a wave analyzer (Hewlett-Packard Model 8553B/8552B) for visual display of the spectra of the fluctuating signal and was recorded on magnetic tape for subsequent analysis by AEDC. A detailed description of the hot-wire anemometer instrumentation is given in Ref. 11.

The a-c response signal from the hot-wire anemometer probe was recorded using the Bell and Howell Model VR3700B magnetic tape machine in the FM-WBII mode. This channel, when properly calibrated and adjusted, has a signal-to-noise ratio of 35 db at 1-v rms output and a frequency response of +1 to -3 db over a frequency range of 0 to 500 kHz. A sine wave generator was used to check each channel at several discrete frequencies, using an rms-voltmeter which was periodically calibrated on the 1-, 10-, and 100-v ranges. The sensor heating current and mean voltage signals from the hot-wire anemometer were also tape-recorded, using the FM-WBI mode. Magnetic tape recordings were made with a tape speed of 120 in./sec.

#### 2.5.4 Pitot Probe Pressure Instrumentation

Pitot probe pressures were measured during surveys of the model boundary layer using a 15-psid Druck transducer calibrated for 10-psid full scale. As the probe was moved across the boundary layer, the small size of the pitot probe (Section 2.4) required a time delay between points in order to stabilize the pressure within the probe tubing between orifice and transducer. In order to reduce the lag time, the pitot pressure transducer was housed in a water-cooled package attached to the trailing edge of the strut on which the probe rake was mounted (Section 2.3). The distance between orifice and transducer was approximately 18 in. The resultant lag time was about 1 sec.

### 3.0 TEST DESCRIPTION

#### 3.1 TEST CONDITIONS AND PROCEDURES

A summary of the nominal test conditions is given below.

<u>M</u>	<u>PT, psia</u>	<u>TT, °R</u>	<u>V, ft/sec</u>	<u>Q, psia</u>	<u>T, °R</u>	<u>P, psia</u>	<u>RE/FT x 10<sup>-6</sup></u>
7.94	225	1310	3856	1.06	98	0.024	1.0
5.96	53.6	850	2992	0.88	105	0.035	1.0

A summary of the test runs for the present measurements using the cooled-wall model is given in Table 3. A complete summary of the various types of measurements made with the sharp- and blunt-cone hot-wall configurations, documented in Refs. 1-3, is presented in Tables 3 and 4 of Ref. 3.

In the continuous-flow Tunnel B, the model is mounted on a sting support mechanism in an installation tank directly underneath the tunnel test section. The tank is separated from the tunnel by a pair of fairing doors and a safety door. When closed, the fairing doors, except for a slot for the pitch sector, cover the opening to the tank, and the safety door seals the tunnel from the tank area. After the model is prepared for a data run, the personnel access door to the installation tank is closed, the tank is vented to the tunnel flow, the safety and fairing doors are opened, the model is injected into the airstream, and the fairing doors are closed. After the data are obtained, the sequence is reversed; the model is retracted into the tank which is then vented to atmosphere to allow access to the model in preparation for the next run. The sequence is repeated for each configuration change.

Probes mounted to the X-Z mechanism (Section 2.3) are deployed for measurements by the following sequence of operations: the air lock is closed, secured over the mechanism, and evacuated; and the access door to the tunnel test section is opened. The various drive systems are used to inject the probes into the test section and position the probes at a designated survey station along the length of the model, the shield protecting the probes is raised exposing them to the flow, and the flow field is traversed in the direction normal to the model surface to selected probe heights. When the traverse has been concluded, the shield is closed over the probes, and the mechanism is repositioned along the model. When the surveys are completed or when a probe is to be replaced, the X-Z Mechanism is retracted from the flow, and the access door is closed. The air lock is then opened to allow personnel access.

The survey probe height relative to the model was monitored using a high-magnification, closed-circuit television (CCTV) system. The video camera was fitted with a telescopic lens system which gave a magnification factor of 20 for the monitor image. The probe and model were back-lighted using the collimated light beam from the Tunnel B shadowgraph system which produced high-contrast silhouettes of the model and probe. The camera was mounted on a horizontal-vertical traversing mount to facilitate alignment of the camera with the probe at various model stations visible through the test section windows. The video camera was interfaced with an image analyzer/digitizer system (IADS) which was used to measure the distance between the probe and model surface using computer-assisted image analysis techniques. The software was designed to locate the lower edge of the probe and the upper edge of the model surface automatically, thus minimizing inconsistencies associated with an operator locating the edges using a cursor. The measurement accuracy was further improved by calibrating the system prior to testing using the automated edge-location technique to locate edges separated by a known distance.



A hardcopy of the video image of the probes and model edge was provided in near real-time, showing, by means of a graphics line, the location of the edges measured and displaying a printout of the measured distance and other pertinent information. The accuracy of this measurement technique was determined to be better than  $\pm 0.0007$ -in. over a range of 0.003 to 0.2 in. under air-off conditions. Provisions were made to determine the magnitude of edge movement caused by probe and model vibrations and to calculate a correction factor for the measurements if required. However, vibrations of the model and probes were negligible when measurements were made under the present test conditions.

The flow-field surveys were accomplished in the following sequence: (1) the model was oriented in roll to avoid interference of the surface instrumentation with the boundary-layer probes, (2) the survey mechanism was positioned at the desired model axial station (XSTA) by the controller operating in either manual or automatic mode and locked in axial position, (3) the survey mechanism was driven downward in the direction normal to the surface by the controller until the "touch-sensor" wire (Section 2.4) attached to the probe shield made contact with the model surface, (4) final adjustments of probe instrumentation were made and the shield was raised, (5) the survey mechanism was driven toward the model surface by the controller until the "touch-sensor" probe (Section 2.3) made contact with the surface, (6) measurements of probe positions relative to the surface and to each other were made using the IADS and the information was manually entered into the data system, (7) the probes were traversed across the flow field in selected increments by the controller in either manual or automatic mode to acquire the desired data, (8) the axial position of the survey mechanism was unlocked and the mechanism was repositioned at the next survey station along the model.

### 3.2 DATA ACQUISITION

The primary test technique used in the present investigation of the effects of model surface temperature upon the initial development of instabilities in a laminar boundary layer was hot-wire anemometry. In addition, mean-flow boundary-layer profile data (pitot pressure and total temperature) were acquired in order to define the flow environment in the vicinity of the hot-wire. All boundary-layer measurements were made above the windward ray of the model. Surface pressures and temperatures on the model were measured to supplement the profile data. The various types of data acquired are summarized in Table 3. Model stations for surveys are also listed in Tables 3a and 3b.

#### 3.2.1 Hot-Wire Anemometry Data

The hot-wire anemometer data acquired during the present testing were of two general categories: (1) continuous-traverse surveys of the boundary layer to map the response of the hot-wire anemometer as a function of distance normal to the surface and (2) quantitative hot-wire measurements using the wire operated at each of a series of

wire heating currents at one or two locations on each profile. The anemometer probes used are identified in Tables 3a and 3b.

Data of the first category were acquired with the hot wire operated using a single heating current, in the present case the maximum (practical) current. The probe was generally translated in a continuous manner from near the model surface outward approximately to the edge of the boundary layer. These data were recorded as analog plots of the hot-wire response (rms of the a-c voltage component) versus probe height normal to the model surface. The plot was used primarily for the purpose of determining the station in the boundary-layer profile where the hot-wire output reached a maximum value.

Quantitative hot-wire data (second category) were acquired at locations determined from the continuous-traverse surveys (first category data). The point of maximum rms voltage output of the hot wire, the "maximum energy point" of the profile, was selected for quantitative measurements at each model station. The quantitative data were acquired using each of a sequence of two or more wire heating currents; one current was nominal-zero to obtain a measurement of the electronic noise of the anemometer instrumentation. Each wire heating current, wire mean voltage (d-c component) and the rms value of the wire voltage fluctuation (a-c component) were measured 11 times using the Tunnel B data system. At the same time, the hot wire parameters were recorded (generally, a 5-sec record duration) on magnetic tape with a tape transport speed of 120 in./sec.

### 3.2.2 Profile and Surface Data

Mean-flow boundary-layer profiles extended from a height of 0.02 in. above the model surface to a distance of at least twice the boundary-layer thickness. A profile typically consisted of 30 to 35 data points (heights). The probe direction of travel was normal to the surface.

Model surface pressures, temperature distributions, and heat-flux distributions were acquired to supplement the boundary-layer surveys. The surface data were obtained throughout the test.

### 3.2.3 Anemometer and Total Temperature Probe Calibrations

The evaluation of flow fluctuation quantitative measurements using hot-wire anemometry techniques requires a knowledge of certain thermal and physical characteristics of the wire sensor employed. In the application of the hot wire to wind tunnel tests, two complementary calibrations are used to evaluate the wire characteristics needed. The first calibration of each hot-wire probe is performed in the instrumentation laboratory prior to the testing: the probe is placed in an oven, and the resistance of the wire is determined as a function of applied wire heating current at several oven temperatures between room temperature and 600°F. The wire reference resistance at 32°F and the thermal coefficient of resistance, also at 32°F, are obtained from the results; the wire aspect (length-to-diameter) ratio is determined,

using the wire resistance per unit length specified by the manufacturer with each supply of wire. Moreover, it has been established that the exposure of the probes to the elevated temperatures of the oven calibration often serves to eliminate probes with inherent weaknesses.

Two hot-wire probes used for flow-field measurements were calibrated in the wind tunnel free-stream flow to obtain both the heat-loss coefficient (Nusselt number) and the temperature recovery factor characteristics of the wire sensor as functions of Reynolds number. The variations of Reynolds number in the free stream were obtained by varying the tunnel total pressure (PT) while holding the tunnel total temperature (TT) at a nominally constant value. The resulting relationships were used to determine the values of the various wire sensitivity parameters required in the reduction of the quantitative measurements.

A calibration of the recovery factor of the total-temperature probe as a function of Reynolds number was made in the free-stream flow of the tunnel test section simultaneously with the calibration of the hot-wire probes. The local total temperature for the probes in free-stream flow was assumed to be equal to the measured stilling chamber temperature, TT (See Section 3.3.4).

### 3.3 DATA REDUCTION

#### 3.3.1 Hot-Wire Anemometer Data

In the present discussion, as it pertains to the reduction of hot-wire anemometer data, only the basic measurements tabulated in the data package that accompanies this report will be considered. (Examples of the tabulations are shown in the Sample Data.) The data processing associated with spectral analysis, modal analysis, and determination of amplification rates of laminar disturbances is beyond the scope of this report. However, extended data reduction of the present hot-wire results to achieve these analyses is planned.

The basic measurements associated with quantitative hot-wire data are the following parameters: wire heating current (CURRENT), wire mean voltage (EBAR), and the rms value of the wire fluctuating response voltage (ERMS). The average value of 11 measurements of each of the three parameters was determined for each nominal wire heating current employed, and the results were tabulated under the designation "DATA TYPE 9" together with certain associated model, flow field, and tunnel conditions. (See Sample 1.)

Free-stream tunnel conditions that are applicable to anemometer and total-temperature probe calibrations are tabulated under the designation "DATA TYPE 6". (See Sample 2.)

#### 3.3.2 Flow-Field Survey Data

The mean flow-field data reduction included calculation of the local Mach number and other local flow parameters, determination of the height of each probe relative to the model surface, correction of the

total-temperature probe using an appropriate recovery factor, definition of the boundary-layer total thickness, and evaluation of the displacement and momentum thicknesses. Sample tabulated data are shown in Sample 3, and typical plotted results are shown in Fig. 6. The data reduction procedures are outlined as follows.

The local Mach number in the flow field around the model was determined using the measured pitot pressure (PP) and the model static pressure (PWL) with the Rayleigh pitot formula.

The height of each probe above the model surface, in the normal direction, was calculated for each point in a given flow-field survey, taking into consideration the following parameters: the initial vertical distance determined from the CCTV image, the distance traversed in the normal direction from the initial position employing the survey probe drive, the lateral displacement of the probe from the vertical plane of symmetry of the model, and the local radius of the model at the survey station.

The height of the pitot pressure probe above the model surface (ZP) was used as the reference for all probes. The recovery temperature measurements (TTTU) of the total temperature probe were used to interpolate a value (TTLU) corresponding to each height of the pitot probe. Correction of the interpolated recovery temperature, using the probe calibration data, was achieved by iteration on the local Reynolds number beginning with the value calculated using the recovery temperature (TTLU) to determine an initial value for the local dynamic viscosity (MUTTL). The iteration was continued until successive values of the "corrected" total temperature differed by no more than 0.1°R. For those surveys wherein the pitot probe was positioned below the total-temperature probe (closer to the model surface), the corrected total temperature at the corresponding pitot probe heights was determined from a second-order curve fit using three points, namely: the model surface temperature (TWL) and the corrected total temperature at the first two probe heights.

The total thickness of the model boundary layer in any given profile was inferred from the profile of the total-temperature probe corrected temperature (TTL). Total temperatures measured above the edge of the boundary layer (in the shock layer) remained constant or essentially independent of the probe height. There was generally a distinct "overshoot" in the total temperature profile immediately before the onset of the constant portion of the profile. The height at which this constant portion of the profile began, the distance normal to the model surface, was defined as the boundary-layer total thickness (DEL). Displacement and momentum thicknesses were determined by integration accounting for the model cone angle and local radius of curvature.

Model surface pressures were measured during mean flow-field surveys, "DATA TYPE 4" (Sample 3). These measurements were made each time that probe data were acquired and the 30 to 35 values for each pressure were averaged. The averaged values are included in the tabulations of DATA TYPE 4.

### 3.3.3 Model Surface Measurements Data

Model surface pressures generally were measured when the survey probe mechanism was located so as not to interfere with the measurements. These data are tabulated under the designation "DATA TYPE 2". (See Sample 4.)

The model surface pressure,  $PWL$ , used in the boundary-layer calculations was determined using a fairing of the pressures measured during the test. (See Fig. 7.) The static pressure was assumed to be constant across the boundary layer to the bow shock and equal to the model surface pressure measured at  $X = 39$ .

### 3.3.4 Total Temperature Probe Calibration Data

The recovery factor  $ETA$  used in reducing the total temperature probe survey data was defined as a function of the local Reynolds number based on probe diameter. Free-stream tunnel conditions that are applicable to the total-temperature probe calibration are tabulated under the designation "DATA TYPE 6" (Sample 2.)

### 3.3.5 Heat-Transfer Data

Data measurements obtained from Schmidt-Boelter gages consisted of the gage voltage ( $E$ ) and the embedded thermocouple temperature ( $TG$ ). The gage output is converted to heating rate by means of a laboratory-calibrated scale factor ( $CSF$ )

$$QDOT = (CSF)(E)$$

The gage wall temperature was obtained from both the embedded thermocouple temperature ( $TG$ ) and the temperature difference ( $\Delta T$ ) across the wafer (See Ref. 10). The temperature difference ( $\Delta T$ ) is proportional to the gage output voltage ( $E$ )

$$\Delta T = (K)(E)$$

The gage wall temperature is

$$TW = TG + \Delta T$$

The heat-transfer coefficient,  $H(TT)$ , based on tunnel stilling chamber temperature was then computed as

$$H(TT) = \frac{QDOT}{(TT - TW)}$$

An example of the tabulated heat-transfer data is shown in Sample 5.

## 3.4 MEASUREMENT UNCERTAINTIES

In general, instrumentation calibrations and data uncertainty estimates were made using methods presented in Ref. 12. Measurement

uncertainty (U) is a combination of bias and precision errors defined as

$$U = \pm (B + t_{95}S)$$

where B is the bias limit, S is the standard deviation, and  $t_{95}$  is the 95th percentile point for the two-tailed Student's "t" distribution, which equals approximately 2 for degrees of freedom greater than 30.

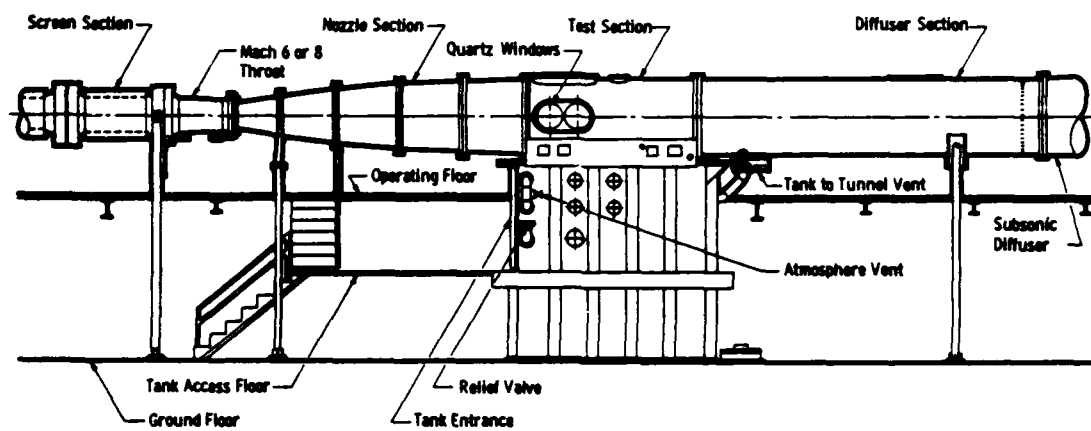
Estimates of the measured data uncertainties for this test are given in Table 2. In general, measurement uncertainties are determined from in-place calibrations through the data recording system and data reduction program. The propagation of the estimated bias and precision errors of the measured data through the data reduction was determined for free-stream parameters in accordance with Ref. 12, and is summarized in Table 4.

#### 4.0 DATA PACKAGE PRESENTATION

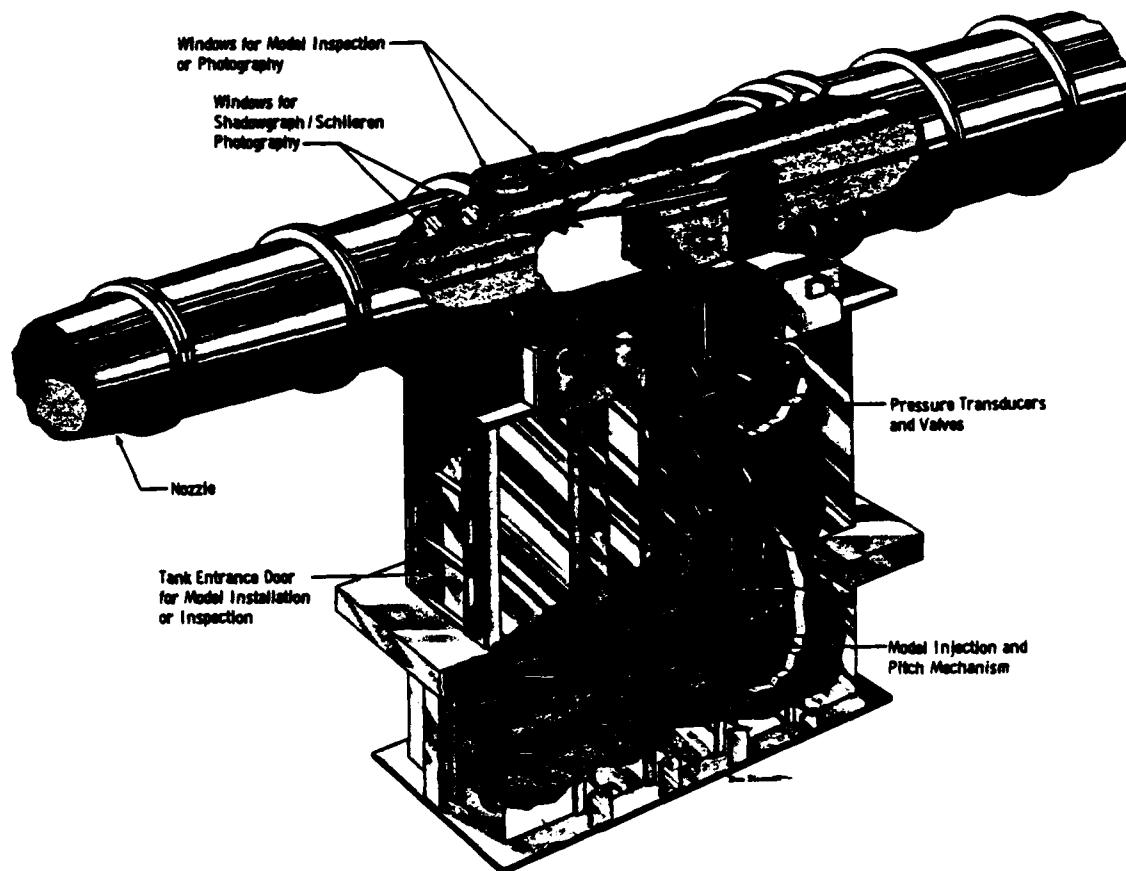
Basic hot-wire anemometer data, boundary-layer profile data, and model surface data from the test were reduced to tabular and graphical form for presentation as a Data Package. Examples of the basic data tabulations are shown in the Sample Data.

## REFERENCES

1. Siler, L. G. and Donaldson, J. C. "Boundary-Layer Measurements on Slender Blunt Cones at Free-Stream Mach Number 8." AEDC-TSR-79-V71 (AD-A085712), December 1979.
2. Donaldson, J. C. and Simons, S. A. "Investigation of the Development of Laminar Boundary-Layer Instabilities Along a Sharp Cone." AEDC-TSR-85-V16 (AD-A159370), April 1985.
3. Donaldson, J. C. and Simons, S. A. "Investigation of the Development of Laminar Boundary-layer Instabilities Along a Blunted Cone." AEDC-TSR-86-V46, December 1988.
4. Stetson, K. F., Thompson, E. R., Donaldson, J. C., and Siler, L. G. "Laminar Boundary-Layer Stability Experiments on a Cone at Mach 8, Part 1: Sharp Cone." AIAA Paper No. 83-1761, July 1983.
5. Stetson, K. F., Thompson, E. R., Donaldson J. C., and Siler, L. G. "Laminar Boundary-Layer Stability Experiments on a Cone at Mach 8, Part 2: Blunt Cone." AIAA Paper No. 84-0006, January 1984.
6. Stetson, K. F., Thompson, E. R., Donaldson J. C., and Siler, L. G. "Laminar Boundary-Layer Stability Experiments on a Cone at Mach 8, Part 3: Sharp Cone at Angle of Attack." AIAA Paper No. 85-0492, January 1985.
7. Stetson, K. F., Thompson, E. R., Donaldson J. C., and Siler, L. G. "Laminar Boundary-Layer Stability Experiments on a Cone at Mach 8, Part 4: On Unit Reynolds Number and Environmental Effects." AIAA Paper No. 86-1087, May 1986.
8. Boudreau, A. H. "Performance and Operational Characteristics of AEDC/VKF Tunnels A, B, and C." AEDC-TR-80-48 (AD-A102614), July 1981.
9. Doughman, E. L. "Development of a Hot-Wire Anemometer for Hypersonic Turbulent Flows." Philco-Ford Corporation Publication No. U-4944, December 1971; and The Review of Scientific Instruments, Vol. 43, No. 8, August 1972, pp. 1200-1202.
10. Kidd, C. T. "A Durable, Intermediate Temperature, Direct Reading Heat-Flux Transducer for Measurements in Continuous Wind Tunnels." AEDC-TR-81-19 (AD-A107729), November 1981.
11. Donaldson, J. C., Nelson, C. G., and O'Hare, J. E. "The Development of Hot-Wire Anemometer Test Capabilities for  $M_\infty = 6$  and  $M_\infty = 8$  Applications." AEDC-TR-76-88 (AD-A029570), September 1976.
12. Abernethy, R. B. et al., and Thompson, J. W. "Handbook Uncertainty in Gas Turbine Measurements." AEDC-TR-73-5 (AD755356), February 1973.



**a. Tunnel assembly**



**b. Tunnel test section**

**Figure 1. AEDC Hypersonic Wind Tunnel (B)**



All dimensions in inches.

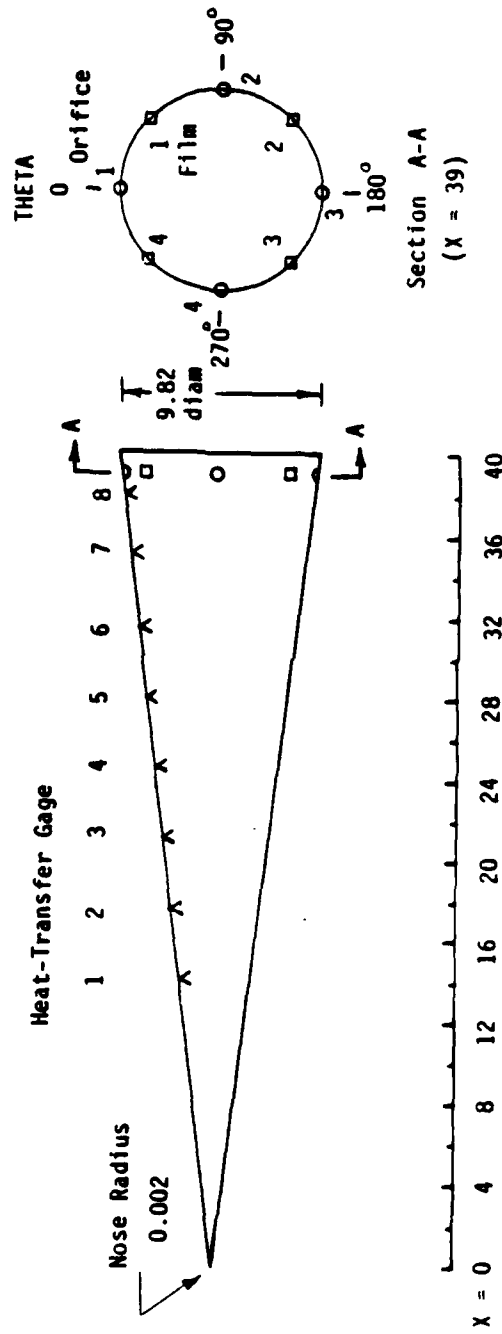


Figure 2. Model Geometry and Instrumentation Locations

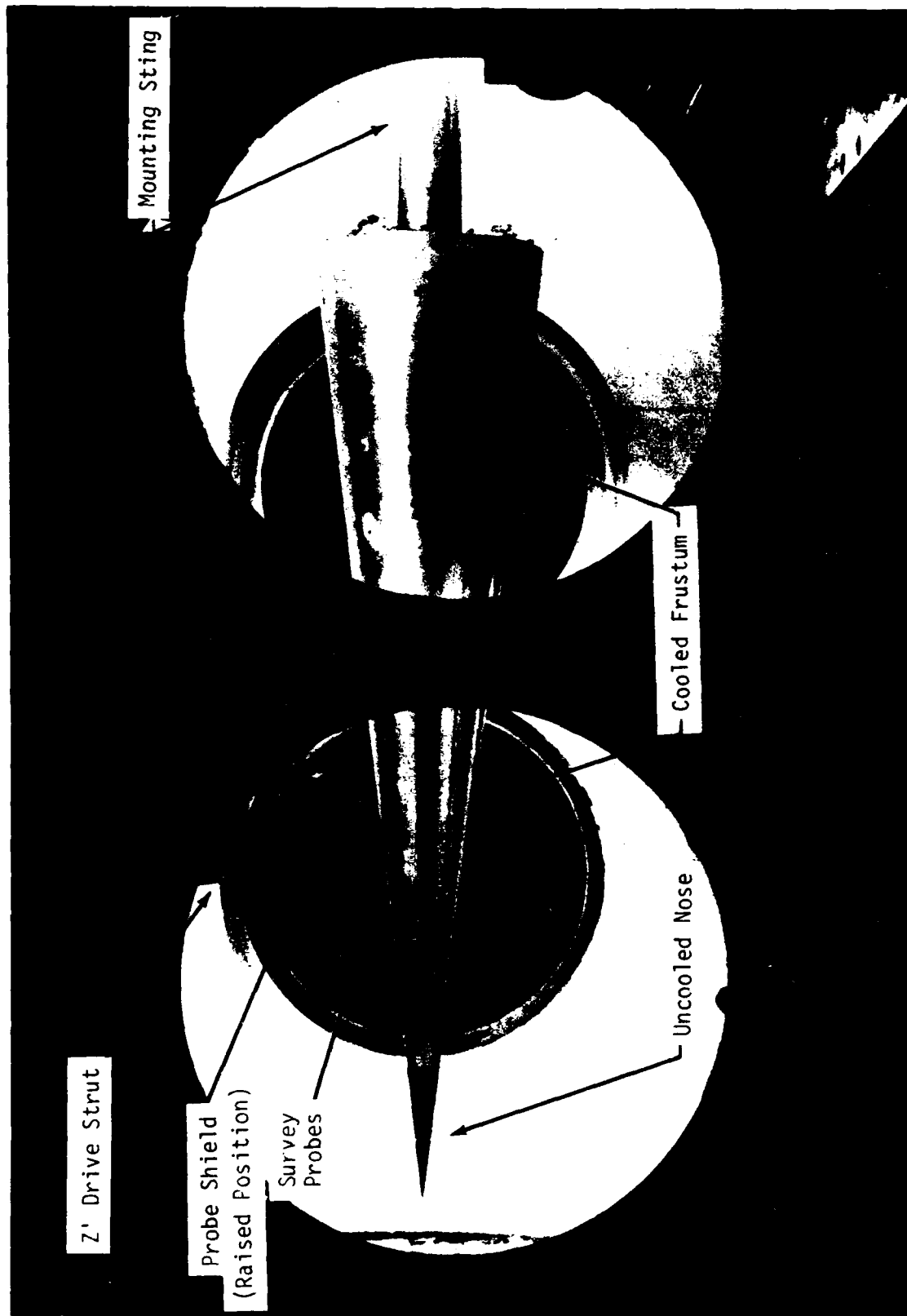
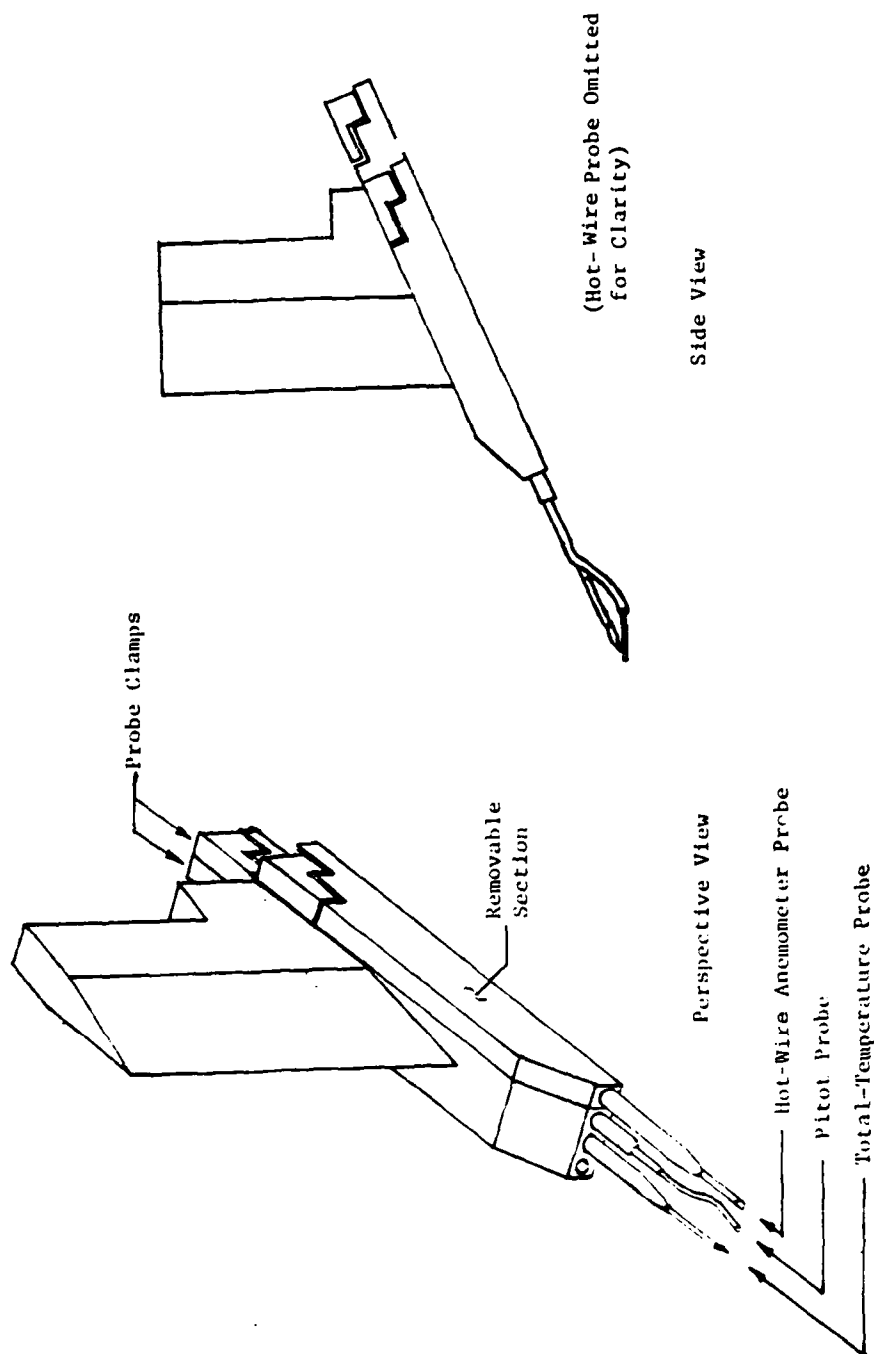
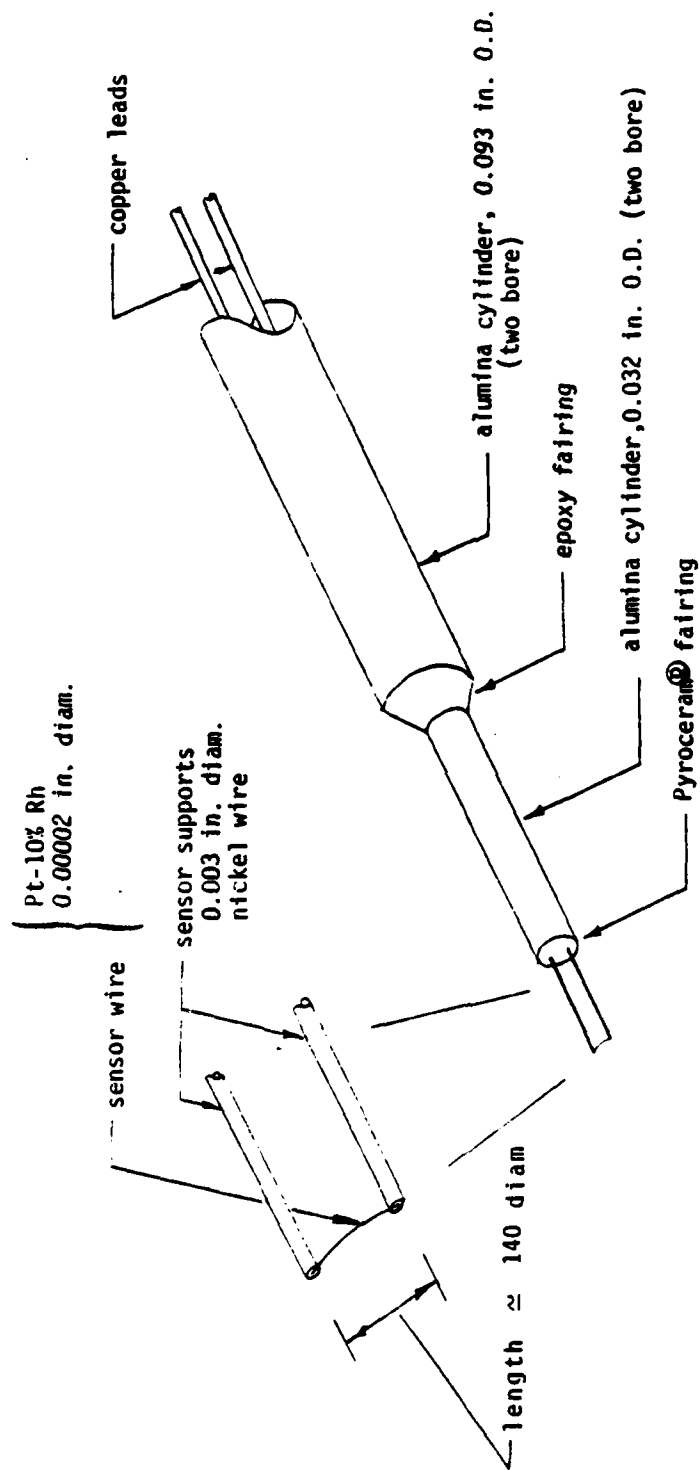


Figure 3. Test Installation

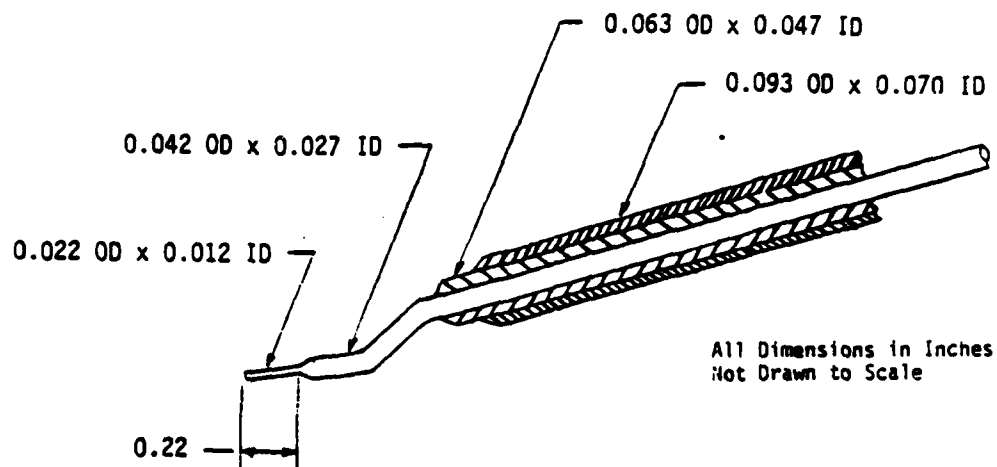


**Figure 4. Survey Probe Rake**

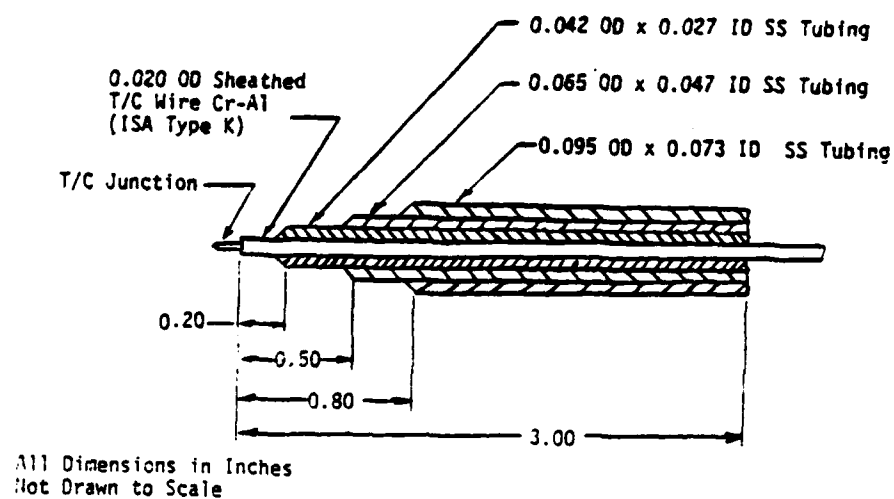


a. Hot - Wire Anemometer Probe

Figure 5. Probe Details



b. Pitot Probe



c. Total-Temperature Probe

Figure 5. (Concluded)

SYMB FIL RUN  
 0 A 144

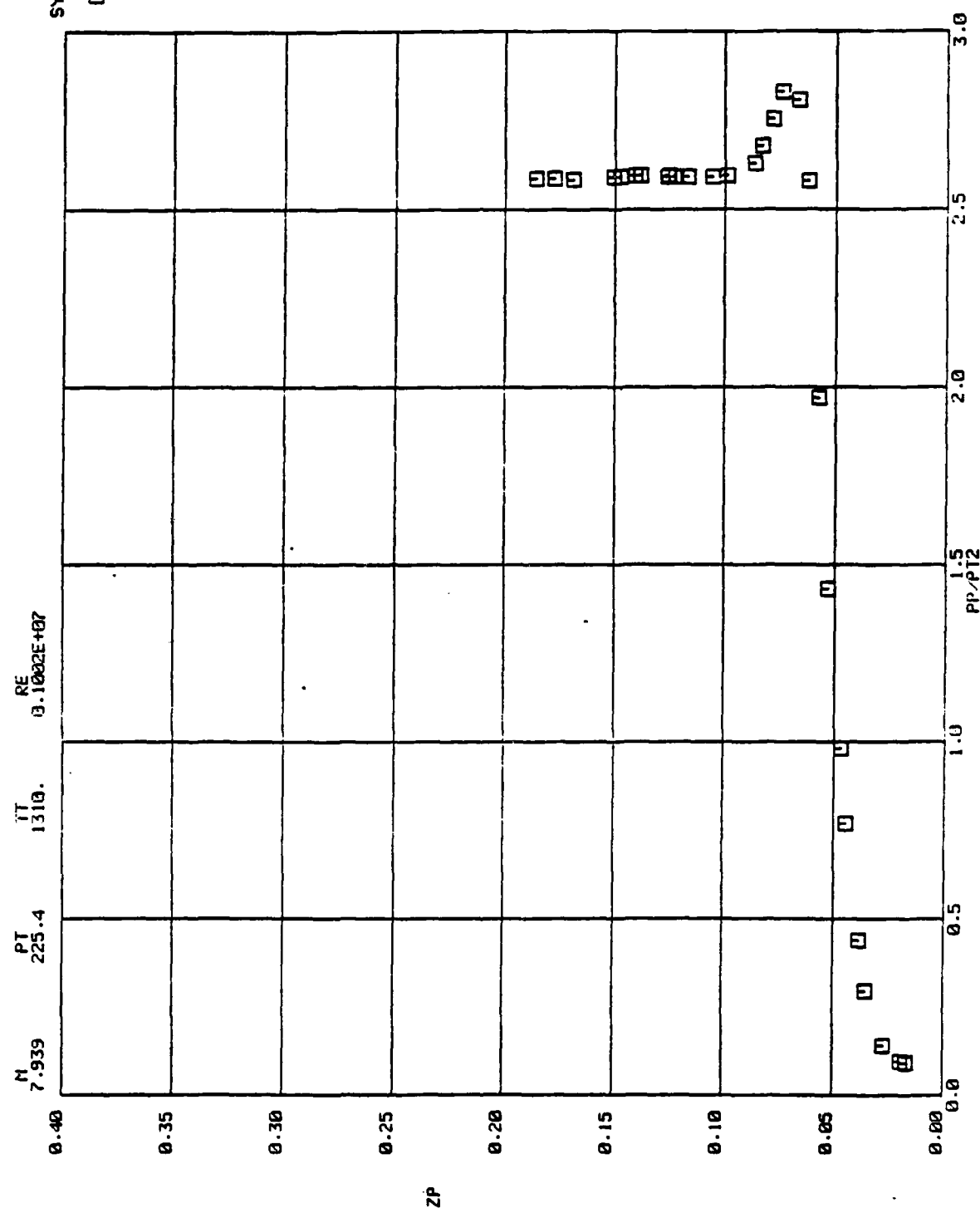


Figure 6. Typical Results of a Mean-Flow Boundary-Layer Survey

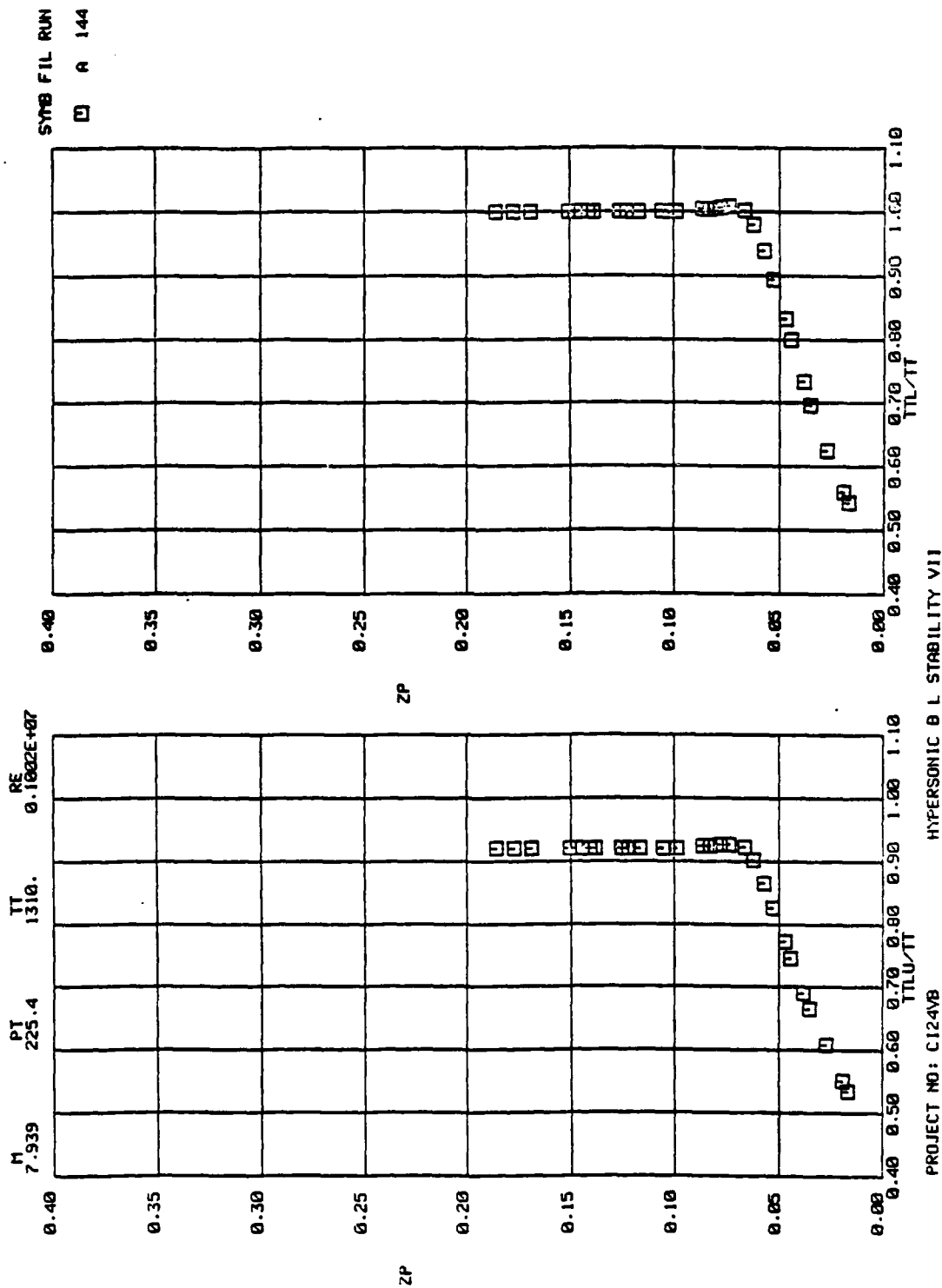


Figure 6. (Continued)

M 7.939    PT 225.4    TT 1310.    RE 0.1002E+07    SYD FIL RUN  
 0.40    0.35    0.30    0.25    0.20    0.15    0.10    0.05    0.00

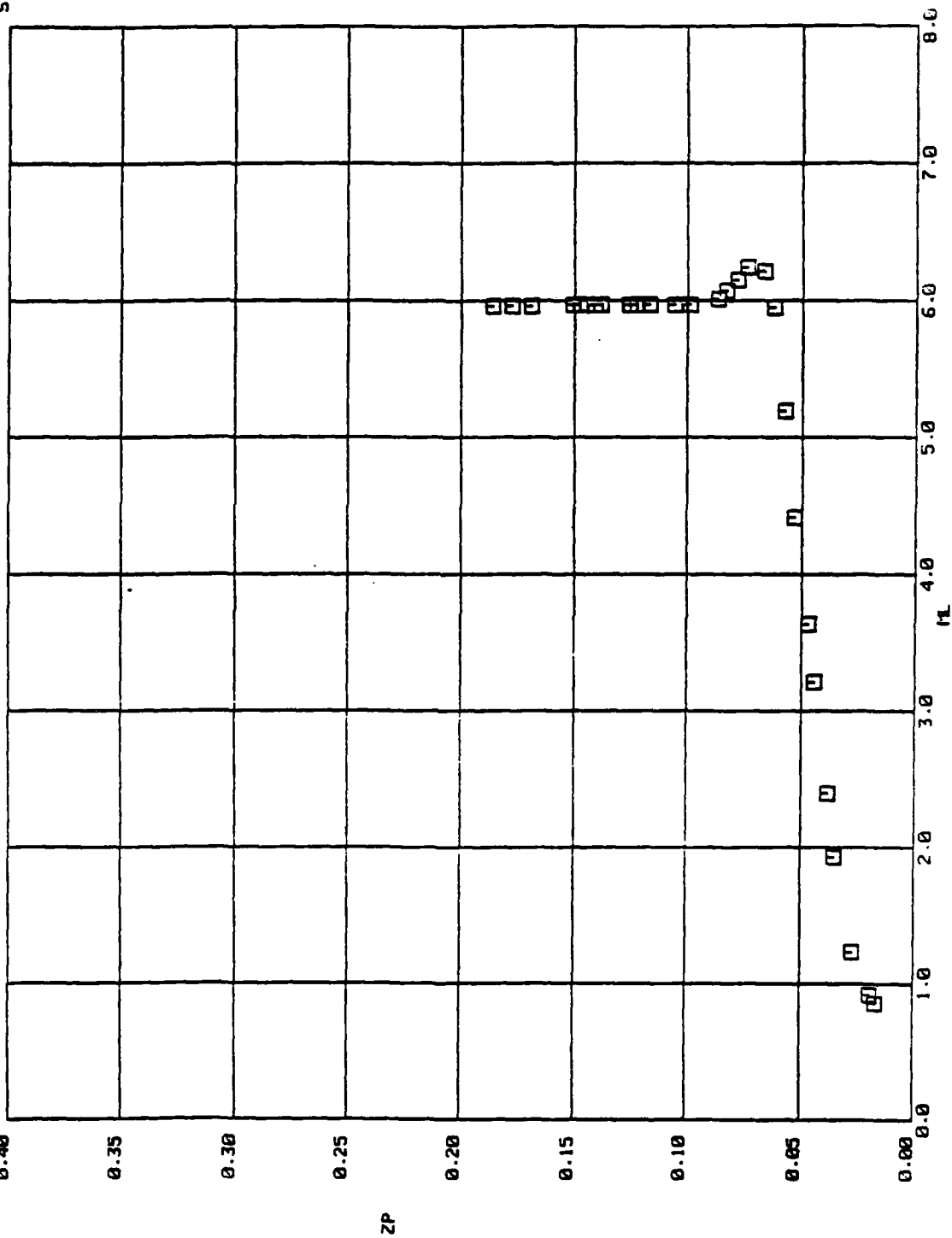


Figure 6. (Concluded)



Note: Open Symbols - Orifice 1

Solid Symbols - Orifice 3

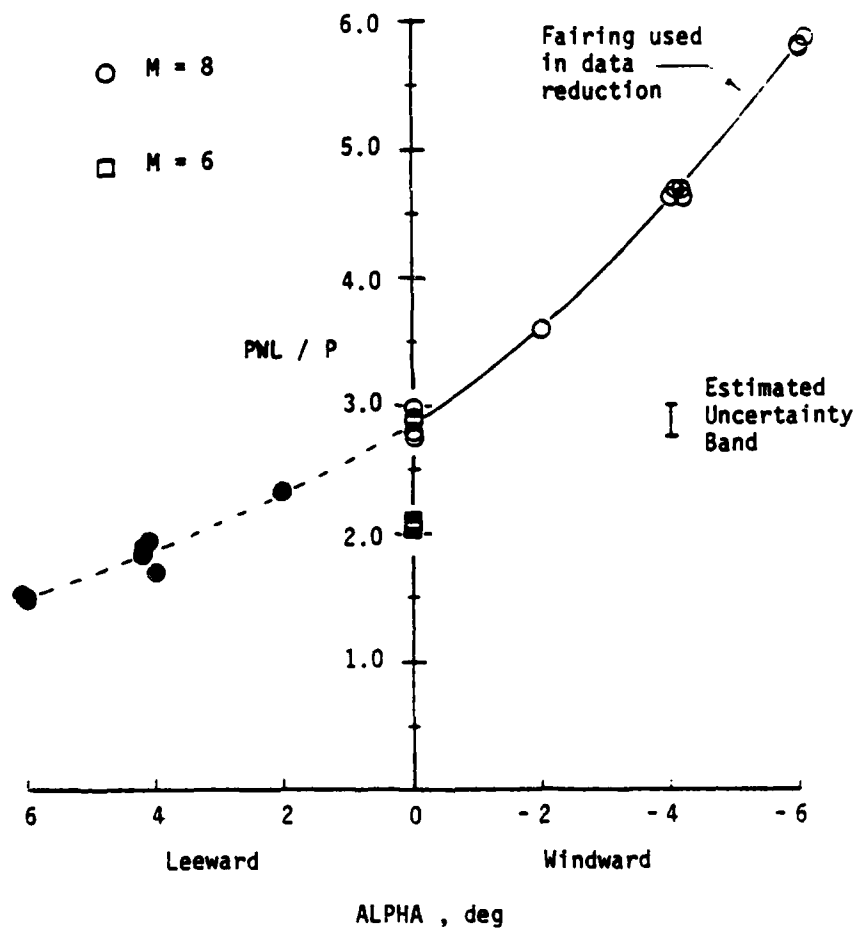


Figure 7. Model Surface Pressure Variation with Angle of Attack

TABLE 1. MODEL INSTRUMENTATION LOCATIONS

PRESSURE ORIFICE LOCATIONS		
ORIFICE	X , in.	THETA , deg
1	39.0	0
2	39.0	90
3	39.0	180
4	39.0	270

SCHMIDT-BOELTER GAGE LOCATIONS		
GAGE	X , in.	THETA , deg
1	14.0	0
2	17.5	0
3	21.0	0
4	24.5	0
5	28.0	0
6	31.5	0
7	35.0	0
8	38.0	0

HOT-FILM ANEMOMETER GAGE LOCATIONS		
GAGE	X , in.	THETA , deg
F 1	39.0	45
F 2	39.0	135
F 3	39.0	225
F 4	39.0	315

TABLE 2. ESTIMATED UNCERTAINTIES OF MEASURED PARAMETERS

Parameter Designation	Steady-State Estimated Measurement*							Range	Type of Measuring Device	Type of Recording Device	Method of System Calibration
	Precision Index (S)		Bias (B)		Uncertainty $\pm (B + 195S)$						
	Percent of Reading	Unit of Measurement	Degree of Freedom	Percent of Reading	Unit of Measurement	Percent of Reading	Unit of Measurement				
Stilling Chamber Pressure (PT), psi		$\pm 0.1$ psi	>30		$\pm 0.1$ psi		$\pm 0.3$ psi	$\pm 0$ to 900 psi	Paroscientific Digiquartz Pressure Transducer	Digital data acquisition system	In-place application of multiple pressure levels measured with a pressure measuring device calibrated in the standards lab
Total Temperature (TT), °F		$\pm 1^\circ\text{F}$ $\pm 1^\circ\text{F}$	> 30 > 30	$\pm 0.375$	$\pm 2^\circ\text{F}$		$\pm 4^\circ\text{F}$ $\pm (375\% + 2^\circ\text{F})$	32 to 530 °F 530 °F to 2300 °F	Chromel-Alumel Thermocouple	Digital Thermometer and Micro Processor Averaged (TTP) Digital Thermometer for Redundant (TTR)	Thermocouple verification of NBS conformity/ voltage substitution calibration
Angle of Attack (ALPHA), deg		$\pm 0.025$ deg	> 30		0°		$\pm 0.05$ deg	$\pm 15$ deg	Potentiometer	Digital data acquisition system/analog-to-digital converter	Heidenhain rotary encoder ROD700 resolution: 0.0006° Overall accuracy: 0.001°
Pitot Pressure (PP), psi		$\pm 0.002$ psi			$\pm 0.010$ psi		$\pm 0.014$ psi	<10 psi	Druck $\pm 15$ psi strain gage transducers	Analog to digital converter/digital data acquisition system	In-place application of multiple pressure levels measured with a pressure measuring device calibrated in the standards laboratory
TTTU, °F		$\pm 1^\circ\text{F}$ $\pm 1^\circ\text{F}$	> 30 > 30	$\pm 0.375$	$\pm 2^\circ\text{F}$		$\pm 4^\circ\text{F}$ $\pm (375\% + 2^\circ\text{F})$	<530 °F <2300 °F	Unshielded Chromel-Alumel Thermocouple	-	Thermocouple verification of NBS conformity/ voltage substitution calibration

\*Reference: Abernethy, R. B. et al and Thompson, J. W. "Handbook Uncertainty in Gas Turbine Measurements." AEDC-TR-73-5, February 1973.

Note: ° Bias assumed to be zero

TABLE 2. CONTINUED

Parameter Designation	Steady-State Estimated Measurement*							Range	Type of Measuring Device	Type of Recording Device	Method of System Calibration
	Precision Index (S)		Bias (B)		Uncertainty $\pm (B + 195S)$						
	Percent of Reading	Unit of Measurement	Degree of Freedom	Percent of Reading	Unit of Measurement	Percent of Reading	Unit of Measurement				
Model Pressure (PM), psi	$\pm 0$	0.0075 psi	> 30	$\pm 1.0$			$\pm (0.0015 \text{ psi} + 1.0\%)$ $\pm (0.004 \text{ psi} + 0.1\%)$ $\pm 0.007 \text{ psi}$	$0 \leq P \leq 0.15 \text{ psid}$ $0.15 \leq P \leq 1.5 \text{ psid}$ $\leq 2.5$	Druck $\pm 1$ psid strain gage transducers  ESPE 2.5 psid strain gage transducer	Analog to digital converter/digital data acquisition system	In-place application of multiple pressure levels measured with a pressure measuring device calibrated in the Standards Lab
Model Temperature (TW), °f		$\pm 1^\circ\text{f}$ $\pm 1^\circ\text{f}$	> 30 > 30		$\pm 2.2^\circ\text{f}$	$\pm 0.375\% \pm 2$	$\pm 4.2^\circ\text{f}$	$< 600^\circ\text{f}$ $< 1600^\circ\text{f}$	Iron-Constantan Thermocouple	Digital data acquisition system analog-to-digital converter.	Thermocouple verification of NBS conformity/voltage substitution calibration
Probe Height Relative to Model Surface (ZP), in		$\pm 0.001 \text{ in.}$	> 30		$\pm 0.002 \text{ in.}$		$\pm 0.004 \text{ in.}$	$< 9.0 \text{ in.}$	Potentiometer and Optical	Digital data acquisition system analog-to-digital converter.	Precision Micrometer
Survey Station (XSTA), in		$\pm 0.011 \text{ in.}$	> 30		$\pm 0.012 \text{ in.}$		$\pm 0.034 \text{ in.}$	$< 26 \text{ in.}$	Potentiometer and Optical Goniacule	Digital Data Acquisition System A/D Converter Optically Positioned Zero	Precision Micrometer
Heat Transfer Gage Output (E), mv	$\pm 0.1$		> 30		$\pm 0.01$		$\pm 0.2\% \pm 0.01$	0 to 10 mv	Millivolt source	Analog to digital converter/digital data acquisition system	Millivolt standard referenced to lab standard
Heat Transfer (QDOT), Btu/ft <sup>2</sup> sec	$\pm 1.5$	$\pm 0.015$	> 30 > 30	2 2		$\pm 5$	$\pm (2\% \pm 0.03)$	$< 1$ 1 to 10	Schmidt-Boelter gage	Analog to digital converter/digital data acquisition system	Radiant heat source and secondary standard
ERMS, mv CURRENT, ma EBAR, mv	$\pm 0.5$ $\pm 0.5$ $\pm 0.5$			0 <sup>+</sup> 0 <sup>+</sup> 0 <sup>+</sup>		$\pm 1$ $\pm 1$ $\pm 1$		$< 1200 \text{ mv}$ $< 5 \text{ ma}$ $< 300 \text{ mv}$	Philco Ford Corp. Model #ADP-12/13 Hot-wire Anemometer System	Digital data acquisition system analog-to-digital converter.	Precision Digital Voltmeter

\*Reference: Abernethy, R. B. et al and Thompson, J. W. "Handbook Uncertainty in Gas Turbine Measurements." AEDC-TR-73-5, February 1973

Note: + Bias assumed to be zero

TABLE 2. CONCLUDED

Parameter Designation	Steady-State Estimated Measurement*							Range + +		Type of Measuring Device	Type of Recording Device	Method of System Calibration
	Precision Index (S)		Bias (B)		Uncertainty ± (B + 195S)							
	Percent of Reading	Unit of Measurement	Degree of Freedom	Percent of Reading	Unit of Measurement	Percent of Reading	Unit of Measurement	Amplitude	Frequency			
Flow Turbulence	Unknown		..	Unknown		Unknown		DC to 1 volt RMS (Heating current up to 2 ma)	DC to 250 KHZ or 500 KHZ (frequency response band determined by filters used)	Hot-wire Anemometer System (20 micro-inch diam)	• Analog data recorded on tape for subsequent playback and reduction • 40 loops of data recorded on digital data acquisition system (AD converter) for each run.	Wire characteristics by oven calibration Heat-transfer characteristics by calibration in tunnel free-stream

\*Reference: Abernethy, R B et al and Thompson, J W "Handbook Uncertainty in Gas Turbine Measurements" AEDC-TR-73-5, February 1973.

\*\* Range of present measurements

TABLE 3. TEST SUMMARY

## a. Hot - Wire Quantitative Run Summary

			X STA, in.																																	
			10 11 12 13 14 15 16 17 18 19 20 21 22 23 24 25 26 27 28 29 30 31 32 33 34 35 36 37																																	
8	16 ↓	0	92 91 90 89 88 87 86 85 84 83 82 81 80 79 78 77 75 74 13 76 **																																	
			31 30 29 28 27 26 25 24 23 22 21 20 19 18 17 16 15 14 13 12 11 10 9 8																																	
			119 117 115 113 111 109 107 106 105 104 103 102 101 100 99 98 97 121 122																																	
			49 48 47 46 45 44 43 42 41 40 39 38 37 36 35 50° 51° 52° 54°																																	
			69 67 65 63 61 59 57 70° 68° 66° 64° 62° 60° 58°																																	
6	10 ↓	0	194 193 192 191 190 189 188 187 186 185 184 183 182 181 180 179 177 176 175 174 173 172 171 170 169 168 167 236 235 234 233 232 231 230 229 228 227 226 225 224 223 222 221 220 219 218 217 216 215 214																																	

Notes \* Measurements at a second peak on the profile of the hot-wire response

\* \* Measurements at seven points on the the hot-wire profile (RUNS 129-135)

TABLE 3. (Continued)

## b. Calibration and Freestream Data Run Summary

M	WIRE NO.	PT psia	CALIBRATION DATA FOR PROBES	HOT-WIRE MEAS. IN FREESTREAM
8	16	225	123	124
		300	125	126
		350	127	—
		200	127	—
		150	127	—
6	10	53	203	202 , 212
		40	204	205
		70	207	206
		100	208	209
		130	211	210

TABLE 3. (Continued)

c. Mean - Flow Boundary - Layer Survey Run Summary

M	ALPHA deg	X STA, in.																
		10	11	12	13	14	15	16	17	18	19	20	21	22	23	24	25	26
8	0																	
6	-4																	
6	-6																	
6	0																	



TABLE 3. (Concluded)

## d. Model Surface Data Run Summary

M	ALPHA deg	PHI deg	TEMP., PRESSURE, HOT-FILM DATA	HEAT-FLUX DATA
8	0	-45	93, 151, 155	94, 150, 156
	0	0	71, 128, 169 *	1, 2, 6, 72, 170
	-2	0	168	3, 167
	-4	-45	95, 148, 173	96, 149, 174
	-4	0	7, 32, 137, 138, 165	4, 166
	-6	-45	172	171
	-6	0	33, 158, 164	5, 157, 163
6	0	-45	195, 213, 237, 244 **	196, 238, 245
	0	0	175	176

Notes: \* Run 55 was for  $M=8$ ,  $ALPHA=0$ ,  $PHI=-4$  deg

\*\* Runs 246 - 258: from  $PT=100$  to 40 psia  
in increments of  $PT$  of 5 psi  
for hot-film data.

TABLE 4. ESTIMATED UNCERTAINTIES OF CALCULATED PARAMETERS									
Parameter Designation	Precision Index (S)			Bias (B)		Uncertainty $\pm (B + 1.95S)$		RE/FT $\times 10^{-4}$ Nom.	MACH, Nominal
	Percent of Reading	Unit of Measurement	Degree of Freedom	Percent of Reading	Unit of Measurement	Percent of Reading	Unit of Measurement		
P, psi	1.23		30	0.05		2.51		1.0	8.0
PT2, psia	0.86			0.05		1.77			
Q, psi	0.85			0.05		1.75			
T, °F	0.36			0.24		0.96			
V, ft/sec	0.04			0.12		0.20			
Rho, lbm/ft³	0.88			0.24		2.00			
MU, lbf-sec/ft²	0.36			0.24		0.96			
M	0.19**			0.		0.38			
RE, per ft	0.53			0.36		1.42			
P, psi	0.55			30	0.19		1.29		
PT2, psia	0.39		0.19			0.97			
Q, psi	0.39		0.19			0.97			
T, °F	0.19		0.24			0.62			
V, ft/sec	0.06		0.12			0.24			
Rho, lbm/ft³	0.43		0.30			1.16			
MU, lbf-sec/ft²	0.19		0.24			0.63			
M	0.08**		0 +			0.16			
RE, per ft	0.33		0.40			1.06			

NOTE: \* Bias assumed to be zero.

\*\* Determined from test section repeatability and uniformity during tunnel calibration.

DATE COMPUTED 23-JUN-88  
 DATE RECORDED 23-JUN-88  
 TIME RECORDED 13:50  
 TIME COMPUTED 01:51:29  
 PROJECT NO V B-32

HYPERSONIC B L STABILITY VII

RUN NUMBER 129 PAGE 1

CONFIG: SHARP 7-DEG CONE (RM - 0.002 IN.)  
 XSTA = 0.20 IN.

DATA TYPE 9  
 HOT WIRE ANEMOMETER DATA

POINT	CURRENT (MAMP)	EBAR (MV)	ERMS (MV)	PT (PSIA)	TT (DEG R)	P (PSIA)	Q (PSIA)	T (DEG R)	RE (PER IN)	ZA (IN.)
1	0.005	0.06	134.89	2.252E+02	1.310E+03	2.398E-02	1.059E+00	9.812E+01	0.343E+04	1.714E-01
2	0.211	3.00	136.94	2.252E+02	1.310E+03	2.398E-02	1.059E+00	9.812E+01	0.343E+04	1.714E-01
3	0.412	5.10	140.93	2.254E+02	1.310E+03	2.401E-02	1.059E+00	9.812E+01	0.343E+04	1.714E-01
4	0.617	7.31	142.08	2.253E+02	1.310E+03	2.400E-02	1.059E+00	9.812E+01	0.347E+04	1.716E-01
5	0.816	9.44	174.45	2.253E+02	1.310E+03	2.400E-02	1.059E+00	9.812E+01	0.347E+04	1.716E-01
6	1.016	11.65	165.10	2.254E+02	1.310E+03	2.401E-02	1.059E+00	9.812E+01	0.347E+04	1.714E-01
7	1.205	13.85	192.54	2.253E+02	1.310E+03	2.399E-02	1.059E+00	9.812E+01	0.347E+04	1.714E-01
8	1.405	16.17	202.69	2.253E+02	1.310E+03	2.398E-02	1.059E+00	9.812E+01	0.347E+04	1.714E-01
9	1.580	18.04	214.51	2.252E+02	1.310E+03	2.398E-02	1.059E+00	9.812E+01	0.347E+04	1.716E-01
10	1.763	19.86	231.55	2.253E+02	1.310E+03	2.399E-02	1.059E+00	9.812E+01	0.347E+04	1.714E-01
11	1.852	21.81	262.51	2.253E+02	1.310E+03	2.399E-02	1.059E+00	9.812E+01	0.347E+04	1.714E-01
12	2.002	23.86	310.84	2.253E+02	1.310E+03	2.400E-02	1.059E+00	9.812E+01	0.347E+04	1.714E-01

ALPHA = 0.02 DEG XC 19.32 (IN)

MACH 7.94

Sample 1. Hot-Wire Anemometer Data

RUN 129

DATE COMPUTED 23-JUN-88  
 DATE RECORDED 23-JUN-88  
 TIME RECORDED 1:3:56  
 TIME COMPUTED 01:51:29  
 PROJECT NO V B-32

CONFIG: SHARP 7-DEG CONE (RM = 0.002 IN.)  
 XSTA = 0.20 IN.

HYPERSONIC B L STABILITY VII  
 RUN NUMBER 129 PAGE 2

DATA TYPE 9  
 HOT WIRE ANEMOMETER DATA

POINT	PT (PSIA)	TT (DEG R)	PWL (PSIA)	TWL (DEG R)	ZP (IN)	PP (PSIA)	ML	TTTTU/TT	TTL/TT
1	2.252E+02	1.310E+03	1.604E-03	5.387E+02	3.400E-02	3.470E+00	4.0983E+01	9.046E-01	6.170E-24
2	2.252E+02	1.310E+03	1.604E-03	5.387E+02	3.400E-02	3.470E+00	4.1007E+01	9.046E-01	6.101E-24
3	2.252E+02	1.310E+03	1.605E-03	5.387E+02	3.472E-02	3.472E+00	4.0979E+01	9.046E-01	6.135E-24
4	2.252E+02	1.310E+03	1.605E-03	5.387E+02	3.472E-02	3.476E+00	4.1019E+01	9.046E-01	6.044E-24
5	2.252E+02	1.310E+03	1.605E-03	5.387E+02	3.472E-02	3.477E+00	4.1019E+01	9.046E-01	6.044E-24
6	2.252E+02	1.310E+03	1.605E-03	5.387E+02	3.400E-02	3.477E+00	4.1019E+01	9.046E-01	6.049E-24
7	2.252E+02	1.310E+03	1.605E-03	5.387E+02	3.400E-02	3.477E+00	4.1019E+01	9.046E-01	6.049E-24
8	2.252E+02	1.310E+03	1.604E-03	5.387E+02	3.472E-02	3.478E+00	4.1035E+01	9.046E-01	6.005E-24
9	2.252E+02	1.310E+03	1.605E-03	5.387E+02	3.400E-02	3.478E+00	4.1022E+01	9.046E-01	6.032E-24
10	2.252E+02	1.310E+03	1.605E-03	5.387E+02	3.400E-02	3.480E+00	4.1034E+01	9.046E-01	5.908E-24
11	2.252E+02	1.310E+03	1.605E-03	5.387E+02	3.400E-02	3.480E+00	4.1034E+01	9.046E-01	5.908E-24
12	2.252E+02	1.310E+03	1.605E-03	5.387E+02	3.400E-02	3.480E+00	4.1034E+01	9.046E-01	5.908E-24

ALPHA = 0.02 DEG XC

MACH 7.94

Sample 1. (Concluded)

RUN 129

DATE COMPUTED 22-JUN-68  
 DATE RECORDED 22-JUN-68  
 TIME RECORDED 6:32:21  
 TIME COMPUTED 06:36:58  
 PROJECT NO V 8-32

HYPERSONIC B L STABILITY VII  
 RUN NUMBER 127 PAGE 1

CONFIG: SHARP 7-DEG CONE (RN = 0.002 IN.)  
 XSTA = 0.00 IN.

DATA TYPE 6: 6 PROBE FLOW CALIBRATION

POINT	M	PI (PSIA)	TI (DEG R)	RE (PER IN)	PP (PSIA)	ML (DEG R)	TTTU (DEG R)	TTTU/TT	ETA	RETD...5
1	7.92	352.1	1312.67	1.542E+06	2.7970	0.1082	1180.6700	0.9971	0.8998	8.390E+00
2	7.92	359.1	1312.67	1.542E+06	2.7981	0.1075	1180.6700	0.9971	0.8998	8.390E+00
3	7.92	197.41	1308.67	8.793E+05	1.6438	0.0341	1181.6700	0.9923	0.8943	6.367E+00
4	7.92	197.21	1308.67	8.795E+05	1.6418	0.0344	1181.6700	0.9936	0.8951	6.367E+00
5	7.92	149.17	1307.67	6.690E+05	1.2556	0.0148	1178.6700	0.9914	0.8933	5.567E+00
6	7.92	148.57	1307.67	6.664E+05	1.2516	0.0134	1178.6700	0.9914	0.8933	5.557E+00

Sample 2. Probe Flow Calibration

RUN 127

DATE COMPUTED 23-AUG-88  
DATE RECORDED 23-JUN-88  
TIME RECORDED 4:20:32  
TIME COMPUTED 21:13:08  
PROJECT NO V 8-32

# HYPERSONIC B L STABILITY VII

RUN NUMBER 144 PAGE 1

CONFIG: SHARP 7-DEG CONE (RN = 0.002 IN.)  
XSTA = 19.00 IN.

## DATA TYPE 4 FLOW FIELD SURVEYS

POINT	PT (PSIA)	TT (DEG R)	PT2 (PSIA)	P (PSIA)	ZP (IN)	PP (PSIA)	PWL (PSIA)	TWL (DEG R)	ZI (IN)	TTU (DEG R)
1	225.41	1309.7	1.965	0.024	0.0168	0.177	0.110	542.3	0.0308	909.7
2	225.11	1308.7	1.963	0.024	0.0190	0.180	0.110	542.3	0.0410	936.7
3	225.11	1308.7	1.963	0.024	0.0269	0.274	0.110	542.3	0.0489	1035.7
4	225.11	1308.7	1.963	0.024	0.0348	0.579	0.110	542.3	0.0568	1130.7
5	225.11	1308.7	1.965	0.024	0.0384	0.863	0.110	542.3	0.0604	1168.7
6	225.21	1308.7	1.966	0.024	0.0441	1.507	0.110	542.3	0.0661	1206.7
7	225.41	1308.7	1.966	0.024	0.0470	1.920	0.110	542.3	0.0690	1212.7
8	225.21	1309.7	1.964	0.024	0.0527	3.812	0.110	542.3	0.0747	1213.7
9	225.31	1309.7	1.965	0.024	0.0571	3.868	0.110	542.3	0.0790	1211.7
10	225.21	1309.7	1.964	0.024	0.0621	5.064	0.110	542.3	0.0841	1208.7
11	225.11	1309.7	1.963	0.024	0.0664	5.500	0.110	542.3	0.0884	1208.7
12	225.21	1309.7	1.964	0.024	0.0736	5.557	0.110	542.3	0.0926	1208.7
13	225.01	1309.7	1.962	0.024	0.0779	4.92	0.110	542.3	0.0958	1208.7
14	225.11	1309.7	1.963	0.024	0.0820	2.57	0.110	542.3	0.1009	1208.7
15	225.21	1309.7	1.963	0.024	0.0855	1.65	0.110	542.3	0.1049	1208.7
16	225.11	1309.7	1.963	0.024	0.0897	1.65	0.110	542.3	0.1085	1208.7
17	225.21	1309.7	1.965	0.024	0.0939	3.094	0.110	542.3	0.1207	1205.7
18	225.31	1309.7	1.965	0.024	0.1059	5.000	0.110	542.3	0.1279	1205.7
19	225.31	1309.7	1.965	0.024	0.1167	5.093	0.110	542.3	0.1307	1205.7
20	225.31	1309.7	1.964	0.024	0.1224	5.091	0.110	542.3	0.1444	1205.7
21	225.21	1309.7	1.965	0.024	0.1260	5.092	0.110	542.3	0.1480	1205.7
22	225.21	1309.7	1.964	0.024	0.1253	5.092	0.110	542.3	0.1473	1205.7
23	225.21	1309.7	1.963	0.024	0.1383	5.092	0.110	542.3	0.1602	1205.7
24	225.11	1309.7	1.964	0.024	0.1404	5.091	0.110	542.3	0.1624	1205.7
25	225.21	1309.7	1.964	0.024	0.1476	5.091	0.110	542.3	0.1656	1205.7
26	225.31	1309.7	1.965	0.024	0.1505	5.088	0.110	542.3	0.1725	1205.7
27	225.31	1309.7	1.964	0.024	0.1692	5.088	0.110	542.3	0.1811	1205.7
28	225.31	1309.7	1.965	0.024	0.1778	5.079	0.110	542.3	0.1888	1205.7
				0.024	0.1864	5.081	0.110	542.3	0.2004	1205.7

PHI = -45.07

M = 7.94  
ALPHA = -4.0 DEG  
DEW = -55. DEG R

## MEAN VALUES

PT = 225.2  
TT = 1309.7  
PT2 = 1.964  
RE = 0.344E+04  
MU = 7.896E-08  
RHO = 6.598E-04

PSIA  
DEG R  
PSIA  
PER IN  
LBF-SEC/FT2  
LBM/FT3

P = 0.0240 PSIA  
PWL = 0.110 PSIA  
TWL = 542.3 DEG R  
V = 3855.1 FT/SEC  
Q = 1.058 PSIA  
T = 98.1 DEG R

## Sample 3. Flow-Field Survey Data

RUN 144

DATE COMPUTED 23-AUG-88  
 DATE RECORDED 23-JUN-88  
 TIME RECORDED 4:20:32  
 TIME COMPUTED 21:13:08  
 PROJECT NO V B-32

HYPERSONIC B L STABILITY VII  
 RUN NUMBER 144 PAGE 2

CONFIG: SHARP 7-DEC CONE (RN = 0.002 IN.)  
 XSTA = 19.00 IN.

DATA TYPE 4  
 FLOW FIELD SURVEYS

LOOP	XP (IN)	PP/PPE	ML	ML/ME (DEG R)	ITLU (DEG R)	TTL (DEG R)	TTL/TTE	TL (DEG R)	UL (FT/SEC)	UL/UE	LRE (PER IN)	LRET (PER IN)
1	0.0168	0.035	0.55E+01	0.143	701.5	712.1	0.544	621.2	1.045E+03	0.201	3.015E+03	2.729E+03
2	0.0190	0.037	0.18E+01	0.154	721.9	734.2	0.560	628.1	1.128E+03	0.204	3.185E+03	2.874E+03
3	0.0269	0.054	1.23E+00	0.206	796.7	818.4	0.625	638.1	1.512E+03	0.457	4.374E+03	3.535E+03
4	0.0348	0.114	1.93E+00	0.323	871.5	913.9	0.698	554.3	2.164E+03	0.582	6.500E+03	5.017E+03
5	0.0384	0.170	2.39E+00	0.401	905.5	959.5	0.732	472.4	2.481E+03	0.793	8.282E+03	7.314E+03
6	0.0441	0.297	3.21E+00	0.510	976.2	1047.2	0.799	342.4	2.901E+03	0.836	9.354E+03	8.057E+03
7	0.0470	0.379	4.42E+00	0.611	1012.2	1090.2	0.832	288.5	3.371E+03	0.891	1.200E+04	1.252E+04
8	0.0527	0.553	5.19E+00	0.741	1082.2	1171.1	0.894	238.2	3.871E+03	0.931	1.586E+04	1.620E+04
9	0.0571	0.761	5.95E+00	0.871	1133.7	1229.7	0.979	186.4	4.371E+03	0.956	1.986E+04	2.058E+04
10	0.0624	1.094	6.21E+00	0.998	1180.3	1281.8	1.002	136.4	4.861E+03	1.008	2.375E+04	2.530E+04
11	0.0664	1.094	6.15E+00	1.042	1217.2	1312.0	1.006	109.1	5.300E+03	1.009	2.757E+04	2.969E+04
12	0.0736	1.063	6.09E+00	1.072	1212.2	1317.4	1.006	85.0	5.730E+03	1.007	3.100E+04	3.368E+04
13	0.0779	1.035	6.00E+00	1.098	1209.1	1313.0	1.003	59.0	6.160E+03	1.004	3.440E+04	3.757E+04
14	0.0829	1.017	5.92E+00	1.108	1205.9	1310.3	1.000	31.2	6.570E+03	1.000	3.767E+04	4.124E+04
15	0.0865	1.003	5.85E+00	1.002	1205.7	1310.0	1.000	161.2	6.960E+03	1.000	4.081E+04	4.482E+04
16	0.0887	1.003	5.79E+00	1.001	1205.7	1310.0	1.000	161.2	7.340E+03	1.000	4.365E+04	4.811E+04
17	0.0859	1.002	5.72E+00	1.001	1205.7	1310.0	1.000	161.1	7.710E+03	1.000	4.603E+04	5.074E+04
18	0.1167	1.002	5.65E+00	1.001	1205.7	1310.0	1.000	161.1	8.080E+03	1.000	4.841E+04	5.359E+04
19	0.1224	1.002	5.58E+00	1.001	1205.7	1310.0	1.000	161.1	8.450E+03	1.000	5.079E+04	5.600E+04
20	0.1260	1.002	5.52E+00	1.001	1205.7	1310.0	1.000	161.1	8.820E+03	1.000	5.317E+04	5.848E+04
21	0.1253	1.002	5.46E+00	1.001	1205.7	1310.0	1.000	161.1	9.190E+03	1.000	5.555E+04	6.097E+04
22	0.1303	1.002	5.40E+00	1.001	1205.7	1310.0	1.000	161.1	9.560E+03	1.000	5.793E+04	6.346E+04
23	0.1494	1.002	5.34E+00	1.001	1205.7	1310.0	1.000	161.1	9.930E+03	1.000	6.031E+04	6.595E+04
24	0.1476	1.001	5.28E+00	1.001	1205.7	1310.0	1.000	161.1	10.300E+03	1.000	6.269E+04	6.844E+04
25	0.1505	1.001	5.22E+00	1.000	1205.7	1310.0	1.000	161.1	10.670E+03	1.000	6.507E+04	7.093E+04
26	0.1692	1.000	5.16E+00	1.000	1205.7	1310.0	1.000	161.1	11.040E+03	1.000	6.745E+04	7.342E+04
27	0.1778	1.000	5.10E+00	1.000	1205.7	1310.0	1.000	161.1	11.410E+03	1.000	6.983E+04	7.591E+04
28	0.1864	1.000	5.04E+00	1.000	1205.7	1310.0	1.000	161.1	11.780E+03	1.000	7.221E+04	7.840E+04

MEAN VALUES  
 PT = 225.3 PSIA  
 TT = 1309.7 DEG R  
 P = 0.0240 PSIA  
 T = 98.1 DEG R  
 N = 7.94 DEG  
 ALPHA = -4.0  
 PHI = -45.07  
 TML/TTE = 0.4140  
 PNL = 0.110  
 TWL = 542.3  
 MEAN VALUES  
 PPE = 5.001E+00 PSIA  
 ME = 5.904E+00 DEG R  
 TTE = 1.310E+03 FT/SEC  
 UE = 0.371E+04 FT/SEC

RUN 144

Sample 3. (Continued)

DATE COMPUTED 23-AUG-88  
 DATE RECORDED 23-JUN-88  
 TIME RECORDED 4:28:32  
 TIME COMPUTED 21:13:08  
 PROJECT NO V B-32

HYPERSONIC B L STABILITY VII  
 RUN NUMBER 144 PAGE 3

CONFIG: SHARP 7-DEG CONE (RN = 0.002 IN.)  
 XSTA = 19.00 IN.

DATA TYPE 4  
 MODEL SURFACE MEASUREMENTS

TAP	X (IN)	THETA (DEG)	PW (PSIA)	PW/P	T/C	X (IN)	THETA (DEG)	TW (DEG R)	TW/TT
1	19.0	0	0.8908	3.7502	1	14.0	0	542.0	0.414
2	19.0	0	0.8942	3.9279	2	17.5	0	542.1	0.414
3	19.0	0	0.8986	2.0280	3	21.0	0	542.2	0.414
4	19.0	0	0.8475	1.9797	4	24.5	0	544.4	0.416
					5	28.0	0	567.3	0.433
					6	31.5	0	555.8	0.424
					7	35.0	0	549.7	0.420
					8	38.0	0	561.2	0.428

HOT FILM GAGE	X (IN)	THETA (DEG)	ERNIS (MV)	EBAR (MV)
F1	19.00	45	-0.0020	11.74
F2	19.00	135	0.0371	11.23
F3	19.00	225	0.0117	0.02
F4	19.00	315	0.0611	12.24

ALPHA = -4.0 DEG  
 PHI = -45.1 DEG  
 XC = 10.997

PT = 225.2 PSIA  
 TT = 1309.7 DEG R  
 W = 7.939  
 RE = 0.100E+07 /FT

TDRK = 548.7 DEG R  
 P = 0.0240 PSIA  
 T = 98.1201 DEG R

Sample 3. (Continued)

RUN 144



HYPERSONIC B L STABILITY VII  
 RUN NUMBER 144 PAGE 4

DATE COMPUTED 23-AUG-88  
 DATE RECORDED 23-JUN-88  
 TIME RECORDED 4:20:32  
 TIME COMPUTED 21:13:08  
 PROJECT NO V B-32

CONFIG: SHARP 7-DEG CONE (RN = 0.002 IN.)  
 XSTA = 19.00 IN.

DATA TYPE 4  
 INTEGRAL EVALUATION

LOOP	ZP/DEL	PP/PPD	ML/MD	TTL/TTD	TL/TD	RHOL/RHOD	UL/UD	MUTL/MUTD	LRE/LRED	DITL/DITD	LREI/LREID
1	0.023E-02	3.489E-02	1.434E-01	5.436E-01	3.047E+00	2.001E-01	2.013E-01	3.300E+00	2.317E-02	2.140E-01	1.102E-01
2	1.018E-01	3.725E-02	1.539E-01	5.005E-01	3.002E+00	2.500E-01	2.015E-01	3.300E+00	2.317E-02	2.140E-01	1.102E-01
3	1.442E-01	5.397E-02	2.064E-01	6.247E-01	3.000E+00	2.500E-01	2.015E-01	3.300E+00	2.317E-02	2.140E-01	1.102E-01
4	1.866E-01	1.140E-01	3.232E-01	6.976E-01	3.000E+00	2.500E-01	2.015E-01	3.300E+00	2.317E-02	2.140E-01	1.102E-01
5	2.059E-01	1.090E-01	4.013E-01	7.325E-01	2.770E+00	3.017E-01	2.015E-01	3.300E+00	2.317E-02	2.140E-01	1.102E-01
6	2.367E-01	2.966E-01	5.379E-01	7.984E-01	2.121E+00	4.714E-01	2.015E-01	3.300E+00	2.317E-02	2.140E-01	1.102E-01
7	2.521E-01	3.794E-01	6.106E-01	8.322E-01	1.470E+00	5.411E-01	2.015E-01	3.300E+00	2.317E-02	2.140E-01	1.102E-01
8	2.830E-01	5.534E-01	7.410E-01	8.940E-01	1.012E+00	6.700E-01	2.015E-01	3.300E+00	2.317E-02	2.140E-01	1.102E-01
9	3.061E-01	9.067E-01	8.711E-01	9.785E-01	0.812E+00	8.012E-01	2.015E-01	3.300E+00	2.317E-02	2.140E-01	1.102E-01
10	3.331E-01	9.067E-01	9.985E-01	1.002E+00	0.812E+00	8.012E-01	2.015E-01	3.300E+00	2.317E-02	2.140E-01	1.102E-01
11	3.562E-01	1.004E+00	1.042E+00	1.002E+00	0.812E+00	8.012E-01	2.015E-01	3.300E+00	2.317E-02	2.140E-01	1.102E-01
12	3.948E-01	1.004E+00	1.042E+00	1.002E+00	0.812E+00	8.012E-01	2.015E-01	3.300E+00	2.317E-02	2.140E-01	1.102E-01
13	4.178E-01	1.004E+00	1.042E+00	1.002E+00	0.812E+00	8.012E-01	2.015E-01	3.300E+00	2.317E-02	2.140E-01	1.102E-01
14	4.449E-01	1.004E+00	1.042E+00	1.002E+00	0.812E+00	8.012E-01	2.015E-01	3.300E+00	2.317E-02	2.140E-01	1.102E-01
15	4.642E-01	1.004E+00	1.042E+00	1.002E+00	0.812E+00	8.012E-01	2.015E-01	3.300E+00	2.317E-02	2.140E-01	1.102E-01
16	5.297E-01	1.004E+00	1.042E+00	1.002E+00	0.812E+00	8.012E-01	2.015E-01	3.300E+00	2.317E-02	2.140E-01	1.102E-01
17	5.602E-01	1.002E+00	1.002E+00	1.000E+00	0.972E-01	1.002E+00	1.000E+00	3.300E+00	2.317E-02	2.140E-01	1.102E-01
18	6.261E-01	1.002E+00	1.002E+00	1.000E+00	0.972E-01	1.002E+00	1.000E+00	3.300E+00	2.317E-02	2.140E-01	1.102E-01
19	6.565E-01	1.002E+00	1.002E+00	1.000E+00	0.972E-01	1.002E+00	1.000E+00	3.300E+00	2.317E-02	2.140E-01	1.102E-01
20	6.762E-01	1.002E+00	1.002E+00	1.000E+00	0.972E-01	1.002E+00	1.000E+00	3.300E+00	2.317E-02	2.140E-01	1.102E-01
21	6.723E-01	1.002E+00	1.002E+00	1.000E+00	0.972E-01	1.002E+00	1.000E+00	3.300E+00	2.317E-02	2.140E-01	1.102E-01
22	7.417E-01	1.002E+00	1.002E+00	1.000E+00	0.972E-01	1.002E+00	1.000E+00	3.300E+00	2.317E-02	2.140E-01	1.102E-01
23	7.533E-01	1.002E+00	1.002E+00	1.000E+00	0.972E-01	1.002E+00	1.000E+00	3.300E+00	2.317E-02	2.140E-01	1.102E-01
24	7.910E-01	1.002E+00	1.002E+00	1.000E+00	0.972E-01	1.002E+00	1.000E+00	3.300E+00	2.317E-02	2.140E-01	1.102E-01
25	8.072E-01	1.001E+00	1.001E+00	1.000E+00	0.985E-01	1.001E+00	1.000E+00	3.300E+00	2.317E-02	2.140E-01	1.102E-01
26	9.075E-01	9.998E-01	9.998E-01	1.000E+00	1.000E+00	9.998E-01	1.000E+00	3.300E+00	2.317E-02	2.140E-01	1.102E-01
27	9.537E-01	9.998E-01	1.000E+00	1.000E+00	1.000E+00	9.998E-01	1.000E+00	3.300E+00	2.317E-02	2.140E-01	1.102E-01
28	1.000E+00	1.000E+00	1.000E+00	1.000E+00	1.000E+00	1.000E+00	1.000E+00	3.300E+00	2.317E-02	2.140E-01	1.102E-01

RHOD = 1.836E-03 LBM/FT3  
 RHOD = 6.931E+00 LBM/SEC-FT2  
 MUTD = 1.200E-07 LBF-SEC/FT2  
 OITD = 1.000E+02 BTU/LBM  
 LREID = 2.476E+04 PER IN

VALUES AT DELTA  
 PPD = 5.081E+00 PSIA  
 MD = 5.9838E+00  
 TD = 1.615E+02 DEG R  
 ITD = 1.310E+03 DEG R  
 UD = 3.715E+03 FT/SEC

DEL = 1.864E-01 IN  
 DEL\* = 4.359E-02 IN  
 DEL\*\* = 3.149E-03 IN  
 LRED = 1.360E+05 PER IN

M = 7.84 DEG  
 ALPHA = -4.0  
 PHI = -45.07

Sample 3. (Concluded)

RUN 144

HYPERSONIC 8 I STABILITY VII

RUN NUMBER 158 PAGE 1

DATA TYPE 2  
MODEL SURFACE MEASUREMENTS

TAP	X (IN)	THETA (DEG)	PW (PSIA)	PW/P
1	39.0	0	0.1302	5.7631
2	39.0	90	0.0622	2.5358
3	39.0	180	0.0353	1.4726
4	39.0	270	0.0626	2.6106

CONFIG: SHARP 7-DEG CONE (RN = 0.002 IN.)  
XSTA = 0.00 IN.

DATE COMPUTED 23-AUG-88  
DATE RECORDED 21-JUN-88  
TIME RECORDED 5:41:28  
TIME COMPUTED 21:20:04  
PROJECT NO V B-32

T/C	X (IN)	THETA (DEG)	TW (DEG R)	1W/TT
1	14.0	0	543.9	0.415
2	17.5	0	545.2	0.416
3	21.0	0	544.6	0.414
4	24.5	0	541.9	0.415
5	28.0	0	543.7	0.413
6	31.5	0	540.9	0.412
7	35.0	0	539.2	0.412
8	38.0	0	540.1	0.410

HOT FILM GAGE	X (IN)	THETA (DEG)	ERMF (MV)	EBAR (MV)
F1	38.00	45	-0.0006	3.97
F2	39.00	135	0.0342	3.39
F3	39.00	225	0.0122	0.02
F4	39.00	315	0.0458	3.54

ALPHA = -0.0 DEG  
PHI = -0.1 DEG

XC = 33.010

PT = 225.1 PSIA  
TT = 1309.7 DEG R  
M = 7.939  
RE = 0.100E+07 /FT

TDRK = 540.7 DEG R  
P = 0.0240 PSIA  
T = 98.1297 DEG R

Sample 4. Model Surface Measurements

RUN 158

DATE COMPUTED: 17-AUG-88  
 TIME COMPUTED: 08:23:51  
 DATE RECORDED: 23-JUN-88  
 TIME RECORDED: 4:49:54  
 PROJECT NUMBER: C124VB

PAGE 1

# HYPERSONIC B L STABILITY VII

RUN NUMBER 149

DATA TYPE: SURFACE HEAT TRANSFER

GAGE NO	X IN	THETA DEG	BTU/FT2-SEC	QDOT	TW DEG.R	HT/FT2-SEC-R	ST(TT)
1	14.00	0.	0.638	0.638	542.41	0.318E-04	1.315E-03
2	17.50	0.	0.529	0.529	543.37	0.900E-04	1.091E-03
3	21.00	0.	0.513	0.513	543.90	0.898E-04	1.059E-03
4	24.50	0.	0.471	0.471	541.68	0.137E-04	0.706E-04
5	28.00	0.	0.415	0.415	542.04	5.412E-04	0.559E-04
6	31.50	0.	0.408	0.408	539.16	5.401E-04	0.584E-04
7	35.00	0.	0.422	0.422	536.65	5.457E-04	0.633E-04
8	38.00	0.	0.495	0.495	544.70	6.475E-04	1.024E-03

SHARP 7-DEG. CONE (RM=0.002 IN.)

PHI = -45.07 DEG  
 M = 7.94  
 ALPHA = -3.98 DEG  
 DEW = -55.97 DEG.F

RUN NUMBER 149

PT = 225.31 PSIA  
 TT = 1369.67 DEG.R  
 P = 0.02 PSIA  
 RE = 1.002E+06 PER FT  
 MU = 7.896E-08 LBF-SEC/FT2

V = 3055.05 FT/SEC  
 Q = 1.059 PSIA  
 T = 90.12 DEG.R  
 PT2 = 1.96 PSIA  
 RHO = 6.601E-04 LBM/FT3

TWIR = 535.67 DEG.R

## Sample 5. Model Surface Heat-Transfer Data